Schweizerische Eidgenossenschaft
Confédération suisse
Confederazione Svizzera
Confederaziun svizra

Federal Department of the Environment,
Transport, Energy and Communications DETEC

Swiss Federal Office of Energy
Energy Research and Cleantech

Final report from 8 August 2025

KYBURZ Direct Battery Recycling

SI/502418-01

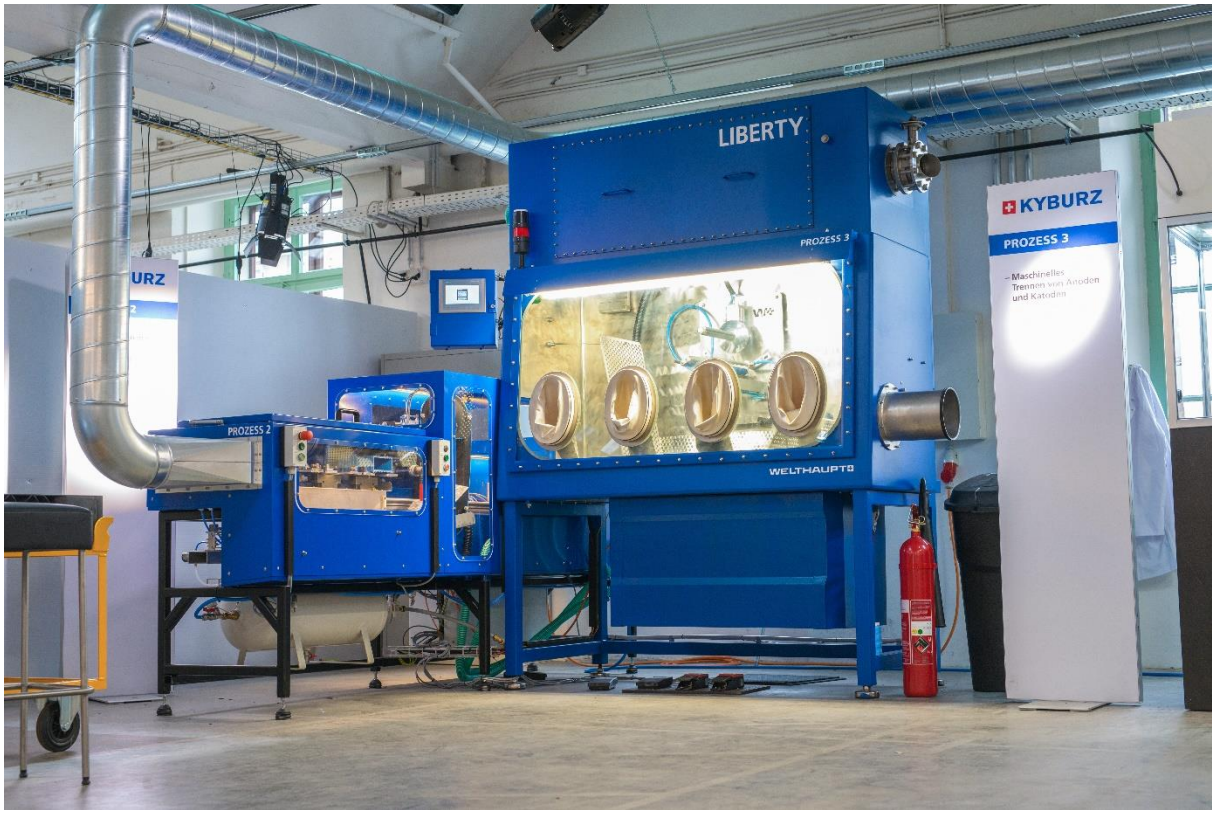

Source: Kyburz Switzerland AG, 2024

Date: 08.08.2025

Location: Bern

Publisher:
Swiss Federal Office of Energy SFOE
Energy Research and Cleantech
CH-3003 Berne
www.energy-research.ch

Subsidy recipients:
Kyburz Switzerland AG
Shedweg 2-8
8427 Freienstein
www.kyburz-switzerland.ch

Empa – Technology and Society Lab (TSL)
Lerchenfeldstrasse 5
9014 St. Gallen
www.empa.ch

Empa – Materials for Energy Conversion Lab (MEC)
Überlandstrasse 129
8600 Dübendorf

Authors:
Andrin Büchel, Empa TSL, andrin.buechel@empa.ch
Martina Serra, Empa TSL, martina.serra@empa.ch
Dawit Ayana, Kyburz Switzerland AG, dawit.ayana@kyburz-switzerland.ch
Nora Bartolomé, Empa TSL, nora.bartolome@empa.ch
Olivier Groux, Kyburz Switzerland AG, olivier.groux@kyburz-switzerland.ch
Kirsten Remmen, Empa TSL, kirsten.remmen@empa.ch
Roland Hischier, Empa TSL, roland.hischier@empa.ch
Edouard Querel, Empa MEC, edouard.querel@empa.ch
Patrick Wäger, Empa TSL, patrick.waeger@empa.ch
Corsin Battaglia, Empa MEC, corsin.battaglia@empa.ch

SFOE project coordinators:
Karin Söderström, karin.soederstroem@bfe.admin.ch
Stefan Oberholzer, stefan.oberholzer@bfe.admin.ch

SFOE contract number: SI/502418-01

The authors bear the entire responsibility for the content of this report and for the conclusions drawn therefrom.

Summary

Lithium-ion batteries (LIB) play a crucial role in the energy transition. End of life (EoL) batteries are shredded and sorted before undergoing pyro- and/or hydrometallurgical treatments. These recycling processes destroy the material morphologies and are energy and chemical intensive. Kyburz Switzerland AG, supported by the Swiss Federal Office of Energy, established an innovative recycling process which allows effective disassembly of LIBs into material fractions of high purity, while keeping the crystallographic structures of the active materials intact. Applying this process to end-of-life batteries, 93 % of the input mass can be recovered for further use including energy recovery. Furthermore, the recycling efficiency of the process was assessed according to the EU Battery Regulation (EU) 2023/1542 guidelines. The KYBURZ process yields an overall recycling efficiency of 67.5 %. In line with the regulation, plastic materials, representing 27.5 % of the total output mass, are excluded from the output fractions, as they are ultimately incinerated, and thus no recycling takes place. The current recycling efficiency exceeds the 65 % target set for the end of 2025. However, the ongoing transition from plastic to metal cell housings is expected to substantially improve recycling efficiency, as metals are considered recyclable output fractions under the regulation.

Moreover, the rate of recovery for copper and lithium as specific target materials in the EU battery regulation were calculated. No copper is lost in KYBURZ' recycling process. Therefore, the copper recovery is 100 % which is above the required 90 % by end of 2027. 67.7 % of the original lithium content can be recovered in the form of $FePO_4$/$LiFePO_4$ active material which is 17.7 % above the required 50 % by end of 2027. Additionally, the process water was identified as an additional source for secondary lithium.

Material characterization of both recovered active materials, i.e. the $FePO_4$/$LiFePO_4$ from the positive electrode and the graphite from the negative electrode, showed intact crystallographic structures. For the positive electrodes, the $FePO_4$/$LiFePO_4$ ratio was 27:73 after processing 90 kg of electrodes. It was found that the cell manufacturer replaced some conductive graphite additive with carbon black between different cell generations. Thereby, the graphite content in the positive electrode was reduced from approx. 7 % to approx. 0.7 %. This highlights potential varieties in output fractions from the process. After efficient separation from the process water, semi-dried graphite from negative electrodes could be collected with a dryness of 70 %. With its removal potential impurities from the process water could be avoided. The discharge capacities of recovered $FePO_4$/$LiFePO_4$ material reached only around 90 mAh/g which corresponds to ca. 70 % of battery grade reference $LiFePO_4$. The recovered graphite reached around 300 mAh/g which corresponds to ca. 85 % of battery grade reference graphite.

A life cycle assessment (LCA) study was conducted to evaluate the ecological impact of KYBURZ' direct recycling process for $LiFePO_4$ - graphite battery cells. The results for the KYBURZ process show a substantially lower carbon footprint compared to hydro- and pyrometallurgical recycling technologies with 0.76 kg CO_2-eq. per kg of recycled battery cell. The other recycling technologies impact with 1.4 – 2.2 kg CO_2-eq. for a hydrometallurgical and 1.8 – 2.4 kg CO_2-eq. for a pyrometallurgical treatment. The disposal of the recovered plastic materials was identified as the major contributor to the environmental impacts due to their incineration. A shift from plastic to metal-based housings could therefore reduce the environmental burden of the KYBURZ recycling process.

In conclusion, an efficient direct recycling process was developed that allows 93 % recovery of the input mass. The guidelines of the EU battery regulation are fulfilled, as the recycling efficiency is over 67.5 %. The recovery rate for copper and lithium are 100 % and 67.7 % respectively. The recovered active material output fractions are crystallographic still in good condition as no side phases were observed. However, the recovered $FePO_4$/$LiFePO_4$ showed a lithium deficit and the recovered graphite indicates that some lithium might still be intercalated in the material. Moreover, the LCA showed that KYBURZ' direct battery recycling process is charged with a lower carbon footprint compared to conventional recycling processes.

Zusammenfassung

Lithium-Ionen-Batterien (LIB) spielen eine entscheidende Rolle in der Energiewende. Am Ende ihrer Lebensdauer (EoL) werden die LIBs vor pyrometallurgischer und/oder hydrometallurgischer Behandlung zerkleinert und sortiert. Diese Recyclingprozesse zerstören die Materialmorphologie und sind energie- sowie chemikalienintensiv. Die Kyburz Switzerland AG hat mit Unterstützung des Bundesamts für Energie ein innovatives Recyclingverfahren entwickelt, welches die LIBs effizient in Materialfraktionen hoher Reinheit zerlegt, wobei die Aktivmaterialien ihre Kristallstrukturen beibehalten. Es können 93 % der Eingangsmasse als Ouputmaterialien zurückgewonnen werden. Die Recyclingeffizienz des Verfahrens wurde gemäss den Vorgaben der EU-Batterieverordnung (EU) 2023/1542 bewertet. Die zurückgewonnenen Kunststofffraktionen, die 27.5 % der Ouputmaterialien ausmachen, können gemäß der Verordnung nicht den Outputfraktionen angerechnet werden, da sie verbrannt werden müssen. Daraus ergibt sich eine Gesamtrecyclingeffizienz von 67.5 %, was über dem bis Ende 2025 geforderten Wert von 65 % liegt. Der derzeitige Trend hin zu metallischen Zellgehäusen, die die Kunststoffgehäuse ersetzen, wird die Recyclingeffizienz erhöhen, da sie für deren Berechnung berücksichtigt werden können.

Ausserdem wurde die Rückgewinnungsrate von Kupfer und Lithium als spezifische Zielmaterialien der EU-Batterieverordnung berechnet. Da während des gesamten Prozesses kein Kupfer verloren geht, beträgt die Kupferrückgewinnung 100 %, was über den bis Ende 2027 geforderten 90 % liegt. 67.7 % des zugeführten Lithiumgehalts können in Form des $FePO_4$/$LiFePO_4$-Aktivmaterials zurückgewonnen werden. Das sind 17.7 % mehr als die bis Ende 2027 geforderten 50 %. Zudem wurde das Prozesswasser als potenzielle zusätzliche Lithiumquelle identifiziert.

Die Materialcharakterisierung zeigte, dass beide zurückgewonnenen Aktivmaterialien – das $FePO_4$/$LiFePO_4$ der positiven Elektrode und das Graphit der negativen Elektrode –intakte Kristallstrukturen aufwiesen. Das $FePO_4$/$LiFePO_4$-Verhältnis war 27:73, selbst nach der Verarbeitung von 90 kg positiver Elektroden. Allerdings wurde festgestellt, dass der Zellhersteller zwischen verschiedenen Zellgenerationen einen Teil des leitfähigen Graphitzusatzes durch Carbon Black ersetzt hat. Dadurch wurde der Graphitanteil von etwa 7 % auf ca. 0.7 % reduziert, was zu Unterschieden in den Outputfraktionen führen kann. Das Graphit der negativen Elektrode konnte nach effizienter Entfernung des Prozesswassers mit einem Trockengehalt von 70 % zurückgewonnen werden. Dadurch wurden zudem potenzielle Verunreinigungen durchs Prozesswasser vermieden. Die Entladungskapazität des zurückgewonnenen $FePO_4$/$LiFePO_4$-Materials erreichte ca. 90 mAh/g, was 70 % des Referenzmaterials entspricht. Das zurückgewonnene Graphitmaterial erreichte ca. 300 mAh/g, was ca. 85 % des Referenzwerts entspricht.

Die ökologischen Auswirkungen des KYBURZ-Recyclingverfahrens für $LiFePO_4$ - Graphit-Batteriezellen wurden mit Hife einer Ökobilanz untersucht. Das KYBURZ-Verfahren weist mit 0.76 kg CO_2-eq. pro Kilogramm rezyklierter Batteriezelle einen deutlich geringeren CO_2-Fußabdruck auf als hydro- und pyrometallurgische Recyclingverfahren. Diese verursachen 1.4–2.2 kg CO_2-eq. im Fall der Hydrometallurgie sowie 1.8–2.4 kg CO_2-eq. im Fall der Pyrometallurgie. Die Entsorgung der Plastikfraktionen wurde als Hauptverursacher der Umweltbelastung identifiziert. Ein Wechsel von Kunststoff- zu Metallgehäusen wird die Umweltbelastung des KYBURZ-Verfahrens somit weiter verringern.

Zusammenfassend wurde ein effizientes Recyclingverfahren entwickelt, das die Rückgewinnung von 93 % der Eingangsmasse ermöglicht. Die Vorgaben der EU-Batterieverordnung werden erfüllt, da die Recyclingeffizienz bei 67.5 % liegt und die Rückgewinnungsraten von Kupfer und Lithium 100 % bzw. 67.7 % betragen. Die zurückgewonnenen Aktivmaterialien behalten ihre Kristallstruktur bei und es wurden keine Nebenphasen entdeckt. Allerdings zeigt das zurückgewonnene $FePO_4$/$LiFePO_4$ ein Lithiumdefizit und im zurückgewonnenen Graphit könnte restliches Lithium interkaliert sein. Zudem zeigte die LCA, dass das Recyclingverfahren von KYBURZ eine geringere CO_2-Belastung aufweist als konventionelle Recyclingverfahren.

Résumé

Les batteries lithium-ion (LIB) jouent un rôle crucial dans la transition énergétique. Les batteries en fin de vie (EoL) seront broyées et triées avant d'être traitées par des procédés pyrométallurgiques et/ou hydrométallurgiques. Ces procédés de recyclage détruisent les morphologies des matériaux et sont intensifs en énergie et en produits chimiques. Kyburz Switzerland AG, avec le soutien de l'Office fédéral de l'énergie, a mis en place un procédé de recyclage innovant, qui permet de désassembler efficacement les batteries lithium-ion en fractions de matériaux d'une grande pureté, tout en conservant intactes les structures cristallographiques des matériaux actifs. Ce procédé permet de récupérer 93 % de la masse d'entrée sous forme de matériaux recyclables. L'efficacité du processus a été évaluée conformément aux lignes directrices du règlement européen sur les batteries (UE) 2023/1542. Les matériaux secondaires en plastique, qui représentent 27.5 % du poids de la cellule, ne sont pas considérés comme des fractions réutilisables dans le cadre de la réglementation, car ils sont incinérés. L'efficacité globale du recyclage est donc de 67.5 %, ce qui est au-delà des 65 % requis pour la fin de l'année 2025. Cependant, la tendance actuelle à remplacer les enveloppes en plastique par des enveloppes en métal améliorera considérablement l'efficacité du recyclage dans un avenir proche.

Le taux de récupération du cuivre et du lithium, qui sont des matériaux cibles spécifiques dans le règlement de l'UE sur les batteries, a été calculé. Aucun cuivre n'est perdu au cours du processus. Le taux de récupération du cuivre est donc de 100 %, ce qui est supérieur aux 90 % requis pour fin 2027. 67.7 % de la teneur initiale en lithium peuvent être récupérés sous forme de matière active $FePO_4$/$LiFePO_4$, soit 17.7 % de plus que les 50 % exigés jusqu'à la fin de 2027. En plus, l'eau de traitement a été identifiée comme une source supplémentaire de lithium secondaire.

La caractérisation des matériaux a montré que la qualité des matériaux récupérés n'est pas affectée par la mise à l'échelle du procédé final. Les deux matériaux actifs récupérés, c'est-à-dire le $FePO_4$/$LiFePO_4$ de l'électrode positive et le graphite de l'électrode négative, présentaient des structures cristallographiques intactes. Le rapport $FePO_4$/$LiFePO_4$ est 27:73 même après le traitement de 90 kg d'électrodes positives. Il a été constaté que le fabricant des cellules a remplacé graphite par carbon black (noir de carbone) comme agent conducteur entre différentes générations de cellules. La teneur en graphite est ainsi passée d'environ 7 % à environ 0.7 %. Cela met en évidence les variations potentielles des fractions de sortie du processus. Le graphite d'électrodes negatives a pu être récupéré semi-sec avec un taux de siccité de 70 % après une separation efficace de l'eau de procédé. Grâce à son extraction, des impuretés potentielles dans l'eau de procédé ont pu être évitées. Le matériau $FePO_4$/$LiFePO_4$ récupéré a atteint environ 90 mAh/g de capacité, ce qui correspond à 70 % du $LiFePO_4$ neuf de référence. Le graphite récupéré a atteint environ 300 mAh/g, ce qui correspond à environ 85 % du graphite de référence.

Une analyse du cycle de vie (ACV) a été menée pour évaluer l'impact écologique du processus de recyclage direct KYBURZ pour les cellules de batteries $LiFePO_4$ - graphite. Les résultats montrent une empreinte carbone nettement inférieure à celle des technologies de recyclage hydro métallurgique et pyrométallurgique, avec 0.76 kg d'équivalent CO_2 par kg d'élément de batterie recyclé. Les autres technologies de recyclage ont un impact de 1.4 à 2.2 kg d'équivalent CO_2 pour un traitement hydrométallurgique et de 1.8 à 2.4 kg d'équivalent CO_2 pour un traitement pyrométallurgique. L'étape finale du processus de recyclage a été identifiée comme le principal facteur contribuant à ces impacts, principalement en raison de l'incinération des composants en plastique du séparateur et du boîtier de la cellule. Le passage de boîtiers en plastique à des boîtiers en métal pourrait donc réduire davantage la charge environnementale du processus de recyclage de KYBURZ.

En conclusion, un processus de recyclage direct a été élaboré qui permet de récupérer 93 % de la masse d'entrée. Les directives du règlement de l'UE sur les batteries sont respectées, puisque l'efficacité du recyclage est à 67.5 % et que le taux de récupération du cuivre et du lithium est de 100 % et de 67.7 %. Les fractions de sortie des matériaux actifs récupérés sont toujours en bon état cristal-

lographique, aucune phase latérale n'ayant été observée. Toutefois, le $FePO_4$/$LiFePO_4$ récupéré présente un déficit en lithium et le graphite récupéré indique qu'une partie du lithium pourrait encore être intercalée dans le matériau. En outre, l'ACV a montré que le processus de recyclage direct des batteries de KYBURZ est chargé d'une empreinte carbone inférieure à celle des processus de recyclage conventionnels.

Main findings («Take-Home Messages»)

- **KYBURZ' DIRECT BATTERY RECYCLING PROCESS ALLOWS EFFICIENT AND SELECTIVE RECOVERY RATES OF 93 %.**
- **KYBURZ' DIRECT BATTERY RECYCLING PROCESS FULFILLS THE GUIDELINES OF THE EU BATTERY REGULATION.**
- **KYBURZ' DIRECT BATTERY RECYCLING PROCESS OFFERS AN INTERESTING SOLUTION FOR LOW VALUE MATERIALS.**
- **KYBURZ' DIRECT BATTERY RECYCLING PROCESS HAS A LOWER CARBON FOOTPRINT IN COMPARISON TO CONVENTIONAL BATTERY RECYCLING PROCESSES.**

Contents

List of abbreviations

CB	Carbon Black
CNT	Carbon Nano Tubes
EDX	Energy-Dispersive X-ray
EF	Environmental Footprint
EoL	End-of-Life
ETOX	Ecotoxicity
EV	Electric Vehicle
GHG	Greenhouse Gas
GWP	Global Warming Potential
HM+	Harvested Material of Positive Electrode ($FePO_4$/$LiFePO_4$)
HM-	Harvested Material of Negative Electrode (graphite)
ICP-OES	Inductively Coupled Plasma Optical Emission Spectroscopy
JRC	Joint Research Center of the European Commission
LCA	Life Cycle Assessment
LCIA	Life Cycle Impact Assessment
LFP	Lithium Iron phosphate, $LiFePO_4$
LIB	Lithium-Ion Battery
LME	London Metal Exchange
MAC	Maximum Allowable Concentration
NMC	Nickel Manganese Cobalt oxide, $LiNi_xMn_yCo_{1-x-y}O_2$
NMR	Nuclear Magnetic Resonance Spectroscopy
PM	Particulate Matter
RU-f	Resource Use - fossil
SEM	Scanning Electron Microscope
SFOE	Swiss Federal Office of Energy
SoH	State-of-Health
SUVA	Swiss Accident Insurance Fund
TGA	Thermogravimetric Analysis
UBP	Umweltbelastungspunkte
VOC	Volatile Organic Compounds
XRD	X-ray Diffraction

1 Introduction

1.1 Context and motivation

Kyburz Switzerland AG, a medium-size enterprise, is seeking to establish an in-house end-of-life (EoL) lithium-ion battery (LIB) recycling plant to recover materials of batteries from their own vehicles. With the funding of the Swiss Federal Office of Energy (SFOE), KYBURZ could advance on a pilot-/demonstration project called "KYBURZ Direct Battery Recycling". The goal of the project was to build a pilot plant for KYBURZ' innovative direct recycling process for LIBs. The novelty of the process is that the battery cells are disassembled in an energy efficient way resulting in material fractions of high purity, while keeping the crystallographic structures of the active material intact (see Figure 1). This potentially allows to reuse these materials in fresh batteries after minor purification and regeneration of the material. In comparison, conventional recycling processes usually shred the cells resulting in a mixture of all cell components that need complex sorting and separation processes to isolate and purify the material fractions. Moreover, hydrometallurgical treatment of the so-called black mass is required to recover precursor substances that can be used for the synthesis of fresh battery active materials. Furthermore, there is currently no economically viable hydrometallurgy process for recovering the materials from $LiFePO_4$ (LFP) – graphite cells, which is KYBURZ' cell chemistry.

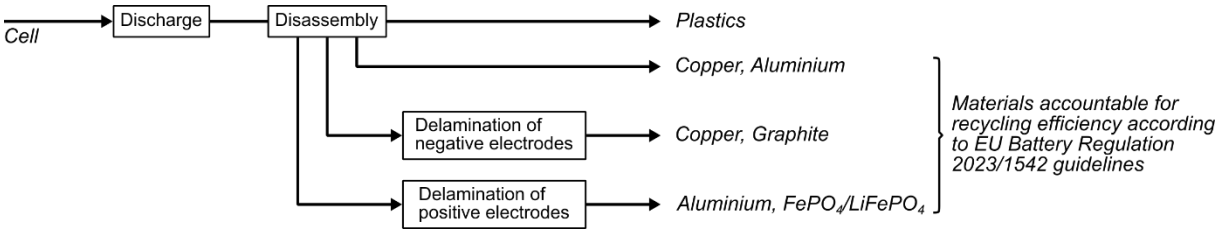

Figure 1: Schematic representation of KYBURZ' direct recycling process. In contrast to conventional recycling processes, no shredding and black mass production occurs and no hydrometallurgical treatment is necessary.

The electrification of transportation is the main driver for the increased demand of LIBs. Europe's EV market is dominated by nickel-manganese-cobalt-oxide (NMC) based cell chemistries [1]. However, LFP chemistries are predicted to gain market shares in the EV market but also in stationary battery energy storage solutions [2]. The increased use of LIBs in turn leads to massive LIB recycling requirements in the near future. In 2023 250 kt of EoL LIBs were recycled, whereas in 2030 about 1'500 kt are expected to be recycled [2]. Recycling of batteries is a long-standing industry that has undergone significant transformations over the years. Historically, the recycling industry was focused on lead-acid and alkaline batteries. However, this has now shifted towards LIBs to meet the evolving market needs as reflected in many headlines and intellectual property announcements [3], [4]. This trend also highlights the growing recognition of LIB recycling as a critical component for a sustainable energy transition.

Due to the dominance of $LiNi_xMn_yCo_{1-x-y}O_2$ (NMC) - graphite cells, the complex and expensive industrial recycling processes were optimized to the recovery of valuable materials nickel and cobalt, which accounts for up to 80 % of the total economic value of the output products. Consequently, NMC batteries have become the primary focus of Europe's recycling industry. From an economic perspective, the recycling of LFP batteries is considered unattractive due to the low market value of the materials. To mitigate this focus, the EU battery regulation demands for ambitious recycling efficiencies and recovery of targets materials such as copper, nickel, cobalt and lithium [5]. However, a notable gap remains specifically for efficient LFP recycling. Because next to the low economic value of LFP, also the phosphates in LFP batteries are specific challenges in hydrometallurgical processing which further diminishes their attractiveness for their industrial recycling. Additionally, Europe's capacity for black mass treatment is not high enough to process needed quantities [6].

Research initiatives, such as those under the Batteries European Partnership (BATT4EU), actively try to address these challenges, emphasizing the importance of innovation in the area of LFP recycling [7]. Also, the KYBURZ Direct Battery Recycling project addresses these challenges by focusing on "direct recycling" as an innovative alternative. This approach relies on mechanical disassembly of battery cells only as far as needed to recover pure material fractions, which offers several key advantages:

- **Recovery of low value materials:** This approach is particularly suited to LFP batteries, whose low material value has historically made them unattractive to recycle in complex and cost intensive processes. Not only LFP but also graphite as another low value material can be recovered and is not lost in the black mass. This leads to a high recycling efficiency of the process.
- **Purity of output fractions:** The process yields pure output fractions, eliminating the formation of black mass. The active materials can be collected separately and without cross contamination. As they maintain their crystal structures, the need of processing of these secondary raw materials is reduced which is beneficial for the environmental footprint if new batteries are produced from these materials.
- **Low environmental footprint:** KYBURZ' recycling process is a more environmentally sustainable alternative to pyro- or hydrometallurgical processes as it does not rely on high energy demand nor heavy use of chemicals.
- **Cost-effective process:** Complex sorting systems and infrastructure for pyro- and hydrometallurgical processing are financially not attractive to process LFP cells. KYBURZ' direct recycling process presents a financially viable solution due to lower investment costs.

In summary, this project aims to overcome economic and technological barriers associated with LFP recycling, providing a sustainable and efficient alternative for handling LFP and graphite materials that has thus far been avoided by traditional recycling approaches.

1.2 Project objectives

In this project, the automation of the water-based electrode delamination unit as an extension of the current pilot plant (phase 1) was demonstrated. Moreover, pure secondary raw materials from LFP cells were recovered. To ensure that the materials used in the batteries remain as intact and pure as possible when they are recovered, the gentle separation of active materials from the current collectors without intermixing the positive and negative electrode active materials is a critical step. The project had the following six objectives: (1) state of health (SoH) estimation and understanding of its impact on the active materials, (2) sustainable management of the electrolyte, (3) effective separation of the active material layers from the current collector foils, (4) development of a process to separate the active materials from the process waters, (5) elemental and structural characterization and electrochemical performance assessment of the recovered material to assess its suitability for reusing in the production of new LFP cells, (6) evaluation of the environmental impact including energy monitoring through life cycle assessment (LCA). To achieve these objectives, the following tasks were addressed within the framework of this project.

1. Provide an overview of the questions related to the SoH required to ensure that the active materials can be recovered and its impact on the resulting material quality.

2. Clarify if washing of the electrode materials in a carbonate bath (e.g., dimethyl carbonate) to wash off the lithium salt is necessary or not. This will also be discussed from the perspective of the reactivity in the process water.

3. Investigate ways for efficient delamination of the active material coatings from the current collector foils. This is necessary to avoid the formation of a black mass that would reduce the value of the low value cell chemistries further. On the contrary, it leads to highly pure material fractions maintaining its highest possible value.

4. Identify and validate a most appropriate system regarding efficiency of active material recovery, water management system and water capturing and reintegrating capability. The separability of the suspension (active materials from water) significantly depends on the nature of the suspension and that of the particles involved. This, however, affects the mechanism(s) that potentially be applied to separate the current collectors (aluminium (Al) and copper (Cu) foils) from the active material suspensions (graphite slurry and LFP flakes). Which methods (filtration, sedimentation, decantation, centrifugation, pressure filter, filter press) or combination of those would efficiently separate the components depends on the nature of the individual materials.

5. Addressing the properties of the recycled active materials is a key indicator of where the KYBURZ direct battery recycling process for LFP batteries should stand in reusing the materials in the production of new cells. Hence, after proper separation of the active materials from the water bath, both graphite and $FePO_4$/$LiFePO_4$ are characterized in view of whether the recovered materials are suitable for reintegration into LFP – graphite batteries. For that, the microstructural, crystallographic and electrochemical properties of the materials were investigated using complementary characterization techniques. This revealed the material qualities achieved at different steps in the recycling process.

6. In order to quantify the environmental impacts of the process, a Life Cycle Assessment (LCA) study was performed to analyze the entire recycling process, taking into account all the stages involved. The use of real data taken either from the facility or experiments will ensure that the assessment is accurate and reliable. The result from this assessment will be compared with the LCA results of other battery recycling processes, including those of state-of-the-art pyro- and hydrometallurgical processes, as well as already published environmental assessments for direct recycling. Overall, the LCA results will provide valuable insights into the environmental performance of the process and identify areas for improvement.

2 Approach, method, results and discussion

2.1 Process-related aspects

The process description starts with a general overview of the process. Each process step is then explained in detail including a mass balance that is normalized to the input of one single cell (sections 2.1.1 & 2.1.2). Then, the detailed descriptions of the different steps are summarized to discuss the complete mass balance of the overall process. These results are then set into context with the requirements of the EU battery regulation (section 2.1.3). Finally, process water analysis and air quality measurements are provided (section 2.1.4).

KYBURZ' recycling process consists of three process steps: first the discharge of cells, second the disassembly of cells into its different components and third the delamination of the active layer coatings from the current collector foils (see Figure 2). The input materials for this process are battery cells. In addition to electricity, process water is needed during the delamination process step. After discharging the cells, disassembly takes place. This results in different output materials: metal connector parts, plastic housing and separator and the positive and negative electrode foils separately. The metals and plastics resulting from disassembly are directly recovered. The electrode foils are further processed in the delamination step where the active layer coatings are separated from the metallic current collector foils.

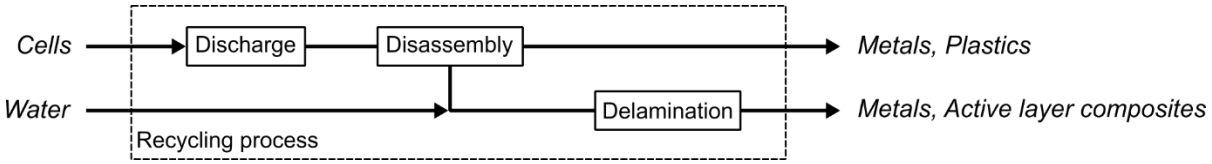

Figure 2: Schematic representation of KYBURZ' recycling process that consists of three steps: discharge, disassembly and delamination. The process was fed with two inputs: the battery cells and water. From this, different output materials were generated. After disassembly, metals and plastics could be recovered and after delamination metals and active layer composites could be recovered. The dashed rectangle defines the system boundaries of the recycling process.

Preparation for recycling is not considered in KYBURZ' recycling process. Preparation for recycling usually covers the disassembly of battery packs into smaller components like modules or individual cells. This practice aligns with the EU's delegated regulation on the methodology to calculate the rates for recycling efficiency and recovery of materials from waste batteries as KYBURZ purchases cells and not the modules [8].

In contrast to conventional recycling processes (i.e. hydrometallurgy and pyrometallurgy), KYBURZ' recycling process provides pure material fractions with minimal contamination instead of black mass. A key advantage of KYBURZ' recycling process therefore is, that it enables a more selective and efficient material recovery. The recovered materials were thoroughly characterized, which is discussed in section 2.2. of this report. The three process steps of Figure 2 are described in detail in the following subsections 2.1.1 and 2.1.2 and quantified with a mass balance normalized to one cell as input fraction.

2.1.1. Discharge and disassembly

The final process setup was tested using EoL LFP prismatic cells (100 - 200 Ah) which have been operated in KYBURZ vehicles for about 7-9 years. Each used cell had a SoH below 60 % and was discharged to 2 V in the first process step. The discharge of the cells was conducted using an in-house developed electrical method. The recovered energy was fed into the grid (compare section 2.3).

After discharge, the cells are semi-automatically disassembled using the LIBERTY 1.0 machine (see front cover). In this machine, the cell casings are opened with subsequent automatic ejection of the

electrode pack using compressed air. The plastic casing of the cell including metallic connector parts are the first output materials. The electrode packs are unrolled by coiling the separator, which consequently is also recovered as output material. Two sharp deflection angles allow to separate the positive and negative electrodes into two containers respectively (see Appendix 7.1). The capacity of LIBERTY 1.0 is estimated to be 200 $^{t}/_{a}$. The collected electrodes are intermediate fractions which are further processed in two separate delamination processes, to produce the final output fractions of the recycling process. These two delamination processes are described in detail in subsection 2.1.2.

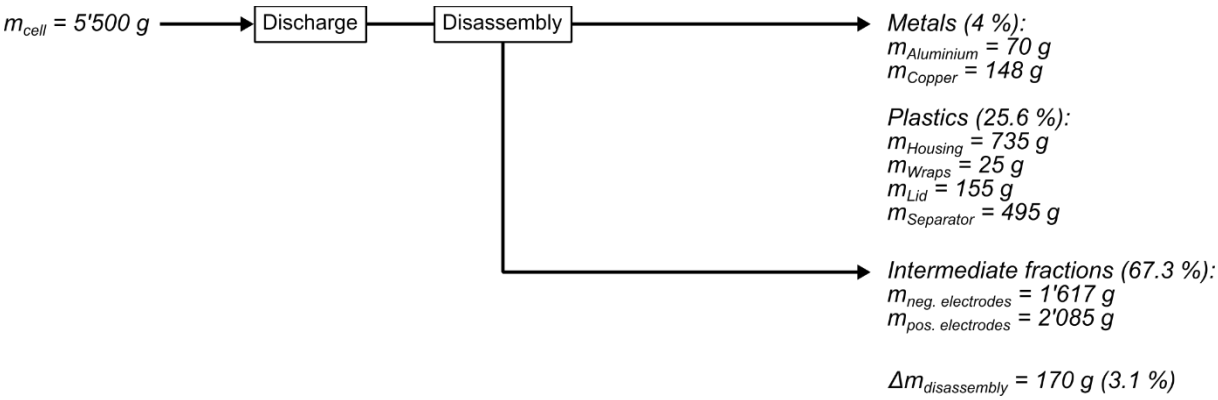

Figure 3: Mass balance of the discharge and disassembly steps normalized to one 180 Ah cell. After disassembly of EoL cells, different metallic and plastic output materials are produced. Moreover, the positive and negative electrodes are recovered as two separate intermediate fractions. The percentages are given as shares of the input material.

In Figure 3 a mass balance of the discharge and disassembly steps corresponding to one 180 Ah cell of 5'500 g as input fraction is depicted. The disassembly resulted in the following output categories: metals, plastics and intermediate fractions. The metallic output materials consisted of the aluminium and copper connector parts that were manually unscrewed from the cropped lid of the cell. In this specific case, the metallic fractions sum up to a mass of 218 g (4% of the input mass). The plastic output materials consist of the housing incl. lid, the wraps that surround the electrode packs and the separator that was extracted by coiling in the LIBERTY 1.0. The plastic fractions sum up to a total mass of 1'410 g (25.6 %). The positive and negative electrodes are individually collected as intermediate fractions (see Appendix 7.1). The total mass of these fractions is 3'702 g (67.3 %). During the disassembly step, a mass difference of 170 g (3.1 %, $\Delta m_{disassembly}$) was measured between the input and output streams. This could be explained by volatile organic solvents from the electrolyte as no loss of solid objects was observable. The measurements of volatile organic components (VOC) support this hypothesis (compare section 2.1.4). The VOCs enter the ventilation system of LIBERTY 1.0 and are filtered with an activated carbon filter system. Another, however most likely negligible contribution could be sawdust from cell opening.

2.1.2. Delamination

For the positive and negative electrodes, two separate delamination processes were developed respectively. This guarantees that cross-contamination between the material fractions is avoided and thus output fractions of high purity are produced. This is a unique characteristic of KYBURZ' recycling process, as conventional recycling processes usually produce a so-called black mass. This black mass results after shredding LIBs and subsequently removing material fractions using complex sorting techniques. The remaining material that cannot be sorted any further gets referred to as "black mass", due to its colour. This black mass usually contains valuable elements such as nickel and cobalt from the active layer coatings. To extract the elements of interest from the black mass, complex hydrometallurgical

processes are necessary to dissolve and precipitate metal salts. As KYBURZ avoids black mass formation with their two separate delamination processes, their recycling process offers an interesting solution for low material value cell chemistries.

The two delamination processes are separately described in detail in the following two subchapters. For both delamination processes real operation mode was simulated by feeding a maximum of 90 kg of positive electrodes and 148 kg of negative electrodes. The mass balances, however, were each normalized to one 180 Ah cell for consistency.

Positive electrode

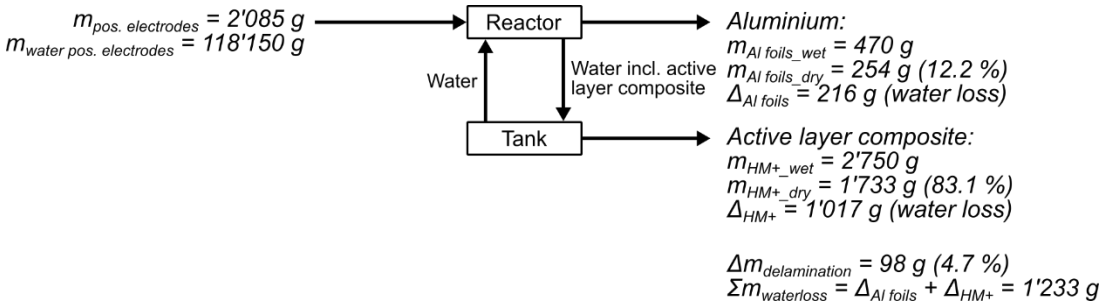

Figure 4: Mass balance of the delamination process of the positive electrodes. The process is fed with positive electrodes and process water. The active material layer (HM+) gets delaminated from the aluminium current collector foils in the reactor and both material fractions could be collected separately. The process water circulated in a closed loop. The water loss ($\Sigma m_{waterloss}$) results in the moisture retained in the output products. The percentages are given as shares of the input material.

The delamination of the $FePO_4$/$LiFePO_4$ active material layer from the aluminium current collector foils is a water-based process (see Figure 4). Hence, the reactor was first filled with deionized water to an initial volume of 850 Liters. The process water was circulated in a closed loop between the reactor and a buffer tank using a pump. After filling with water, the positive electrodes were manually and continuously fed into the reactor at a rate of 15 kg/h. The process water remained in a closed-loop system. The same water was reused for consecutive batches, and even after processing 90 kg of feed no decline in delamination performance was observed.

Within the reactor the active material layer is delaminated from the current collector foils. The retention time of the electrodes in the reactor was set until complete delamination was achieved. During delamination the adhesion between the active layer coating and the aluminium foil could be overcome so that the coating delaminated as complete and intact layers. Nevertheless, mechanical wear also disrupted cohesive forces within the active material coating, generating smaller flakes (compare section 2.2.2).

After delamination, the rinsed aluminium foils were discharged from the reactor and collected in a designated container. When processing the intermediate fraction $m_{pos.\ electrodes}$ (2'085 g per 180 Ah cell) a dry mass of aluminium foil $m_{Al\ foils\_dry}$ (254 g, 12.2 %) was recovered. No visual loss or disintegration of the aluminium foil was observed. The discharged process water, including the active layer flakes was collected in the buffer tank below. From this tank, the process water was pumped back into the reactor. In total, a dry mass (m_{HM+_dry}) of 1'733 g (83.1 %) of $FePO_4$/$LiFePO_4$ containing active layer composite was harvested. After harvesting, the process water was returned into the reactor being available for the next batch. The only water loss during the delamination process resulted from moisture retained on the aluminium foils and the active material. The total water loss ($\Sigma m_{waterloss}$) was 1'233 g which had to be replenished.

Calculating the mass balance between the input mass and output mass, a difference of $\Delta m_{delamination}$ (98 g, 4.7 %) was observed. This mass is assumed to be active material layer that is withhold in the circulating process water. Thus, no material was lost, as it can be collected in a later batch. However, this material remaining in the process water limits the overall efficiency of the recycling process. After

collecting the remaining material in a later batch, KYBURZ estimates that the overall losses of material will account for only 0.5 % of active material layer.

Negative electrode

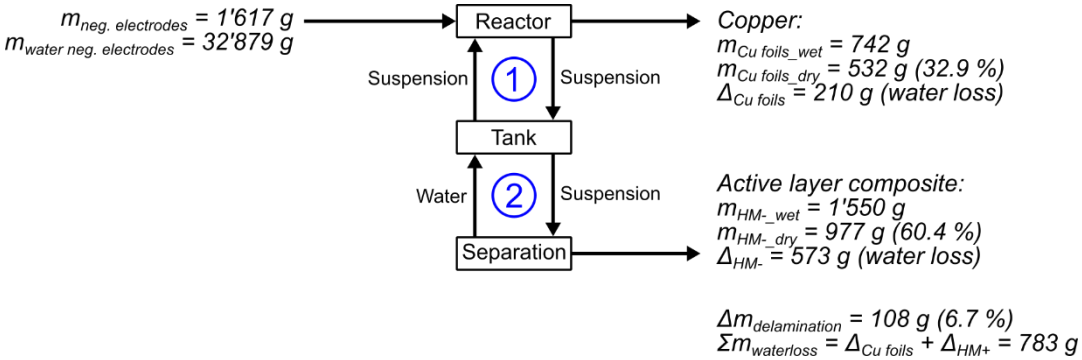

Figure 5: Mass balance of the delamination process of the negative electrodes. The process is fed with negative electrodes and process water. The process water is kept in a closed loop and circulates in the two cycles (indicated in blue). In the first cycle, the active layer (HM-) gets delaminated from the copper current collector foils. The resulting suspension gets filtered through a separation unit in the second cycle. The process water is then returned to the first cycle. The water loss ($\Sigma m_{waterloss}$) results in the moisture in the output products. The percentages are given as shares of the input material.

The delamination of the graphite active material layer from the copper current collector foils is conducted in a water-based process (see Figure 5). Hence, the reactor was first filled with deionized water to an initial volume of 550 Liters. The process water circulated in a closed loop between the reactor and a buffer tank using a pump. The negative electrodes were then fed manually and continuously into the reactor at a rate of 30 kg/h. The water was circulated in a closed loop and the only water loss occurred due to moisture retained in output fractions. The water can be reused for several batches. After processing 148 kg of electrodes, the delamination performance remained unaffected.

Within the reactor the active material layer is delaminated from the current collector foil. The retention time of the electrodes in the reactor was set until complete delamination was achieved. During delamination not only the adhesion between the active layer coating and the copper foil could be overcome but also the cohesion within the active layer coating itself. Hence, other than the flakes of the positive electrodes, a visually homogeneous suspension was formed in which the graphite particles or small particle aggregates are suspended in the process water. An exothermic reaction could be observed and the pH of the process water increased. This can be explained by the exothermic nature of the reaction between lithium and water:

$$2\ Li_{(s)} + 2\ H_2O_{(l)} \xrightarrow{\Delta H = -222\ {}^{kJ}/_{mol}} 2\ LiOH_{(aq)} + H_{2\,(g)}$$

The lithium source for this reaction is expected to come from the lithium that is integrated in the solid electrolyte interface (SEI) on the graphite particle surface [9].

After delamination, the washed copper foils were discharged from the washing system and collected in a designated container. When feeding the intermediate fraction $m_{neg.\ Electrodes}$ (1' 617 g per 180 Ah cell) a dry mass of copper foil $m_{Cu\ foils\_dry}$ (532 g, 32.9 %) could be recovered. No visual losses or disintegration of the copper foils was observed. The discharged process water suspension containing the active material particles was collected in a buffer tank below. The suspension was then filtered through a separation unit. The filtrate was pumped back into the tank from which it was circulated again through the reactor. The batchwise harvested material had a dry mass of m_{HM-_dry} (977 g, 60.4 %) of graphite containing active layer composite. The only water loss during the process occurred due to the retained moisture on the copper foils and the active material. The total water loss ($\Sigma m_{waterloss}$) was 783 g which

needed to be replenished. The dryness of the harvested graphite material was 70 % after applying compressed dry air during process water separation.

Calculating the mass balance between the input mass and output mass, a difference of $\Delta m_{delamination}$ (108 g, 6.7 %) was observed. This mass is assumed to be active material layer that is retained in the circulating process water. Thus, no material was lost, as it can be collected in a later batch. However, this material remaining in the process water limits the overall efficiency of the recycling process. After collecting the remaining material during a later batch, KYBURZ estimates that the overall losses of material will account for only 1 % of active material layer.

2.1.3. Recycling efficiency

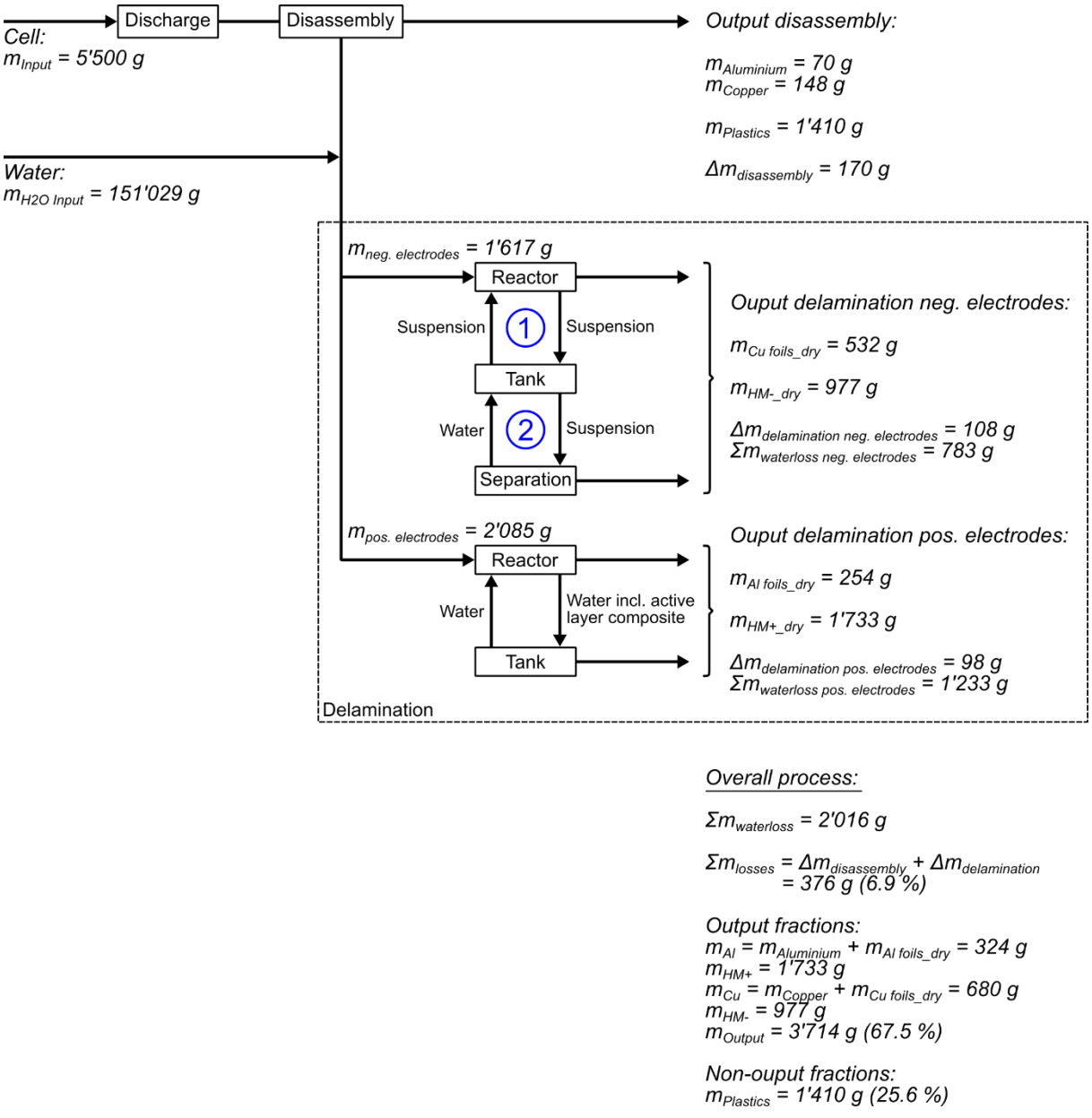

Figure 6: Mass balance from the complete recycling process normalized to the input of one single 180Ah cell. Both delamination processes are shown within the dashed rectangle. The process was fed with two input materials: the battery cell and process water. From this, different output materials were generated.

After disassembly, metals and plastics could be recovered and after delamination metals and active layer materials could be recovered. Each process step is charged with a loss that consist of the difference between input mass minus the resulting output mass ($\Delta m_{...} = m_{input} - m_{output}$). The process water was circulated in closed loops and the only water loss resulted from the moisture retained in the output products. The percentages are given as shares of the input material.

To summarize, KYBURZ' direct battery recycling process consists of three process steps: first the discharge of cells, second the disassembly of cells into its different components and third the delamination of the active layer coating from the current collector foils (see Figure 6). The process is fed with two inputs: the battery cells (m_{input} = 5'500 g) and process water. From this, the output materials m_{Al}, m_{HM+}, m_{Cu}, m_{HM-} and $m_{Plastics}$ are generated. The total mass of the recovered materials sums up to $m_{recovered\ total} = m_{Plastics} + m_{Output}$ = 5'124 g. Consequently, 93 % of the input mass can be recovered, and are available for further use.

However, in the EU battery regulation, not all the recovered materials can be accounted as "output fractions" for the calculation of the recycling efficiencies. Therefore, KYBURZ' recycling process is set into context to the demands of the regulation. The methodology for calculating the rate of recycling efficiency for waste batteries in relation to a recycling process is defined in a commission delegated regulation supplementing the EU battery regulation [8]. For lithium-based batteries it is defined as:

$$rRE = \frac{\sum m_{output}}{m_{input}} \times 100, [mass\ \%]$$

where:

rRE = rate of recycling efficiency for waste batteries in relation to a recycling process [in mass %],

m_{output} = output fractions taken into account for recycling per calendar year [in tonnes],

m_{input} = input fractions per calendar year [in tonnes].

The EU battery regulation demands ambitious targets for recycling efficiency and recovery of materials. By 31.12.2025 the recycling efficiency for lithium-based batteries needs to be at least 65 % by average weight. No later than 31.12.2030 a 70 % recycling rate needs to be achieved [5]. The rate of recycling efficiency is calculated based on the chemical composition of the input and output fractions. Below, these two fractions are defined for the KYBURZ' recycling process.

The input fraction m_{input} is the mass of waste batteries prepared for recycling and entering the waste battery recycling per calendar year, measured in tonnes. This includes casings and cables that are integral parts of the batteries available on the market. As KYBURZ purchases their batteries as individual cells, the input fraction is the mass of a single 180 Ah cell with which the recycling process was tested. The facility is still in pilot phase, therefore the mass is just considered as the mass of a single cell in grams and not in tons per calendar year. This simplification should not affect the calculation of the recycling efficiency as the input and output masses are expected to scale linearly by the same factor when extrapolating to a full calendar year. Hence, the input fraction was a 180 Ah LFP cell with a measured mass of m_{input} = 5'500 g.

Intermediate fractions are masses of waste batteries which are neither an input nor an output fraction but are destined for subsequent step(s) in the waste battery recycling. These subsequent steps have the aim of converting the intermediate fractions into one or more output fractions. Hence, the positive and negative electrodes recovered from cell disassembly are considered as two individual intermediate fractions of $m_{pos.\ electrodes}$ = 2'085 g and $m_{neg.\ electrodes}$ = 1'617 g.

Output fractions m_{output} are materials, substances or products that are recovered from recycling of the input fractions and will be used for their original purpose or other purposes but excluding landfill construction, backfilling operations, reprocessing into materials that are to be used as fuels and energy recovery. Even though the regulations are tailored more to the conventional recycling processes such

as pyro- or hydrometallurgical recycling routes that generally focus on the recovery of high value materials, also accounting of low value materials is accepted. This is in favour of KYBURZ' recycling process as it is tailored to the recovery of mostly low value materials from their in-house LFP cell supply. The low value materials for m_{input} and m_{output} are oxygen, carbon from carbon sources at cell level, iron from iron sources at cell level, phosphorous, chlorine and sulphur. Starting 1 January 2030, carbon and iron originating at the cell level must also be included when calculating recycling efficiency. As illustrated in Figure 6 KYBURZ' recycling process yields four different output materials that can be accounted for as output fractions. These output materials are aluminium, copper, graphite and $FePO_4$/$LiFePO_4$ active layer materials. Thereby the total output fraction sums up to m_{output} = 3'714 g.

$$rRE = \frac{\sum m_{output}}{m_{input}} \times 100\ \% = \frac{3'714g}{5'500g} \times 100\ \% = 67.5\ \%$$

This results in a recycling efficiency of 67.5%. Therefore, KYBURZ recycling process already fulfils the required 65 % of the regulation. However, it must be noted that the material losses in the recycling process only account for $rLoss = \frac{\sum m_{losses}}{m_{input}} \times 100 = \frac{376}{5'500} \times 100 = 6.8\ \%$ which is mostly due to active material retained in the process water. This material is, however, not lost per se but might still be recovered in a following batch as the process water circulates in multiple cycles. Moreover, the plastic fractions can be recovered as separate material fractions in KYBURZ' recycling process and account for 25.6 % of the input mass. But since the plastic fraction recovered by KYBURZ will be incinerated, they are not accountable as output fractions. This will likely change in the near future, as there is a trend away from plastic cell housings toward metal housings. These metal housings could then be counted as output fractions, resulting in a significantly higher recycling efficiency (compare section 2.2.5). Additionally, these calculations start with the cell mass, in contrast to conventional processes, which include the battery casing, cables, and other integral components. This emphasizes the margin resulting from cell recycling disproportionally high in comparison to the conventional processes where cell masses are only a share of the whole battery mass (m_{input}).

2.1.4. Process water analysis and air quality measurements

Process water analysis

Previous water analysis from small scale experiments at an earlier stage of the project were conducted by the Office for Waste, Water, Energy, and Air of the Canton of Zürich (AWEL). They measured a copper concentration in the negative electrode process water of 3.47 mg/l, exceeding the legal disposal limit of 1 mg/l [10]. Additionally, the lithium concentrations in the negative and positive electrode process waters were found to be 175 mg/l and 44 mg/l, respectively. It is important to note that the concentration values mentioned above originated from small batches.

New measurements were now conducted on the final process setup where the process water had been circulated as explained in section 2.1.2 and electrodes were continuously fed into the system. In total, three water samples were collected for the analysis. Two from the delamination process of the positive electrodes, once after processing 26 kg and once after 90 kg of positive electrodes. The third water sample was collected from the separation unit after delaminating 148 kg of negative electrodes. All three samples were analysed using inductively coupled plasma optical emission spectroscopy (ICP-OES) for elemental composition and nuclear magnetic resonance (NMR) Spectroscopy for molecules characterization.

Table 1: Elemental analysis from the positive and negative electrode process water samples. From the positive electrode delamination, water was collected after processing 26 kg and 90 kg respectively. The process water of the negative electrode delamination was collected from the separation unit after processing 148 kg of negative electrodes. PW is an abbreviation for process water.

Sample	Aluminium [mg/l]		Copper [mg/l]		Iron [mg/l]		Lithium [mg/l]	
	mean	SD	mean	SD	mean	SD	mean	SD
Positive electrode PW – 26 kg	1.63	0.23			49	1.17	116	2.08
Positive electrode PW – 90 kg	9.07	0.15			148	2.11	419	5.66
Negative electrode PW – 148 kg			8.93	0.84	15	0.75	1'322	33.9

The elemental analysis showed that the primary metallic impurities present in the process water were aluminium, copper, iron, and lithium (see Table 1). The concentrations of these elements increased with the number of processed positive electrodes. Especially the high lithium concentration increased further from 116 mg/l to 419 mg/l. Since the delamination process was still effective after processing 90 kg of positive electrodes, it is expected that the same water can be used to delaminate additional electrodes. Consequently, the lithium concentration in the solution is assumed to increase further with larger batch sizes. Also, iron and aluminium concentrations were quantified at 148 mg/l and 9 mg/l, respectively. Although the water sample was centrifuged and only the supernatant was directly introduced into the ICP-OES, some suspended particles might have remained in the supernatant due to incomplete sedimentation and were subsequently introduced into the system. The negative electrode process water showed a significantly higher lithium concentration of 1'322 mg/l, along with minor impurities of iron (14.5 mg/l) and copper (8.93 mg/l). Copper impurities might originate from current collector corrosion during use of the cells [11].

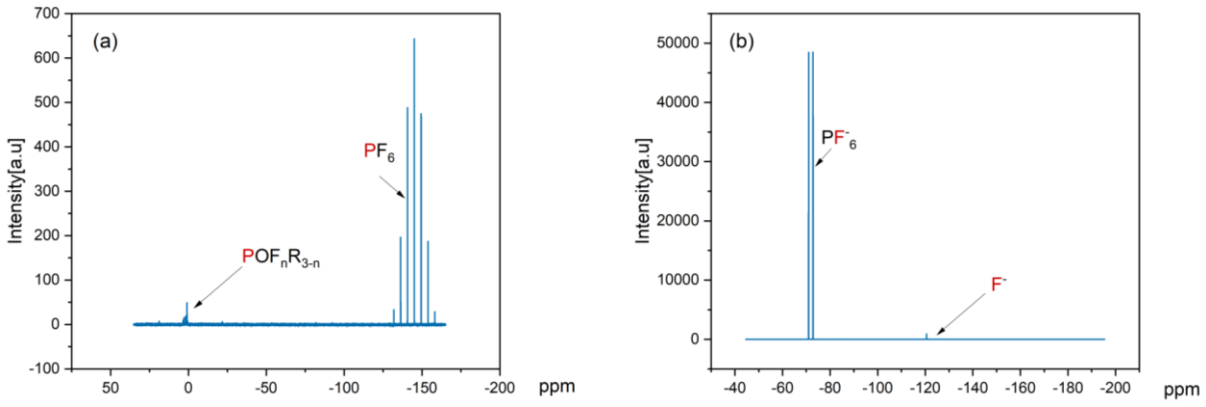

Figure 7: NMR results for the positive electrode process water: (a) ^{31}P NMR spectrum showing the septet of the fluorine coordination around -150 ppm and trace degradation products around 0 ppm, (b) ^{19}F NMR spectrum showing the doublet couple with phosphorous and the single F^- anion.

Possible molecular impurities in the water samples were characterized using NMR. The main molecule observed in the ^{31}P NMR spectrum exhibits a septet around -150 ppm, indicating coupling of the phosphorus atom with six equivalent fluorine atoms (see Figure 7, a). This is further supported by the 19F NMR spectrum, which shows a doublet at approximately -70 ppm (see Figure 7, b), consistent with fluorine coupling to a single phosphorus atom. These results confirm that the primary species present

is the PF_6^- anion, corresponding to the original anion from the electrolyte salt. Additionally, trace degradation products were detected in both NMR spectra. In the ^{31}P NMR spectrum, signals observed around 0 ppm suggest the presence of POF_nR_{3-n} compounds. The ^{19}F NMR spectrum shows a characteristic fluoride singlet near -120 ppm, indicating the presence of free fluoride ions. No signal corresponding to HF, which typically appears around -180 ppm, was detected. This absence is consistent with the chemical behaviour of $LiPF_6$ in aqueous conditions because the PF_6^- anion does not undergo hydrolysis in pure water [12]. And even if $LiPF_6$ hydrolyses to form HF, this is a weak acid ($pK_a \sim 3.17$) and remains stable only under acidic conditions. Under neutral or basic conditions, like the situation of the process water samples with a pH ~ 9, HF readily dissociated to form fluoride ions at unproblematic concentrations.

Table 2: ^{31}P, ^{19}F, and ^{7}Li NMR summary results for the positive and negative electrode delamination process waters. 50 mM $LiPF_6$ in water was used as reference sample for the quantification of the concentrations. PW is an abbreviation for process water.

Sample	Species	Concentration [mM]		
		^{31}P NMR	^{19}F NMR	^{7}Li NMR
Positive electrode PW – 26 kg	PF_6^-	5.1	6.3	
	POF_nR_{3-n}	1.4		
	F^-		0.34	
	Li^+			12.86
Positive electrode PW – 90 kg	PF_6^-	34.53	31.43	
	POF_nR_{3-n}	6.8	0.05	
	F^-		1.27	
	Li^+			54.77
Negative electrode PW – 148 kg	PF_6^-	28.73	22.9	
	POF_nR_{3-n}			
	F^-		1.4	
	Li^+			193.15

Using a reference sample with 50 mM $LiPF_6$ in water allowed integrating the peaks from both the reference and actual samples for a quantitative analysis listed in Table 2. For the positive electrode process water PF_6^- concentrations of 31 - 34 mM, lithium concentrations of 55 mM, and fluoride concentrations of 1.27 mM were quantified after processing 90 kg of electrodes. The concentrations of all species increased with the number of processed electrodes. For the negative electrode process water PF_6^- concentrations of 23 - 29 mM, lithium concentrations of 193 mM, and fluoride concentrations of 1.4 mM were detected in the water after the separation unit. When converted to mg/l units using the molar mass of lithium (6.94 g/mol), the lithium concentration determined by NMR are 382 mg/l for the positive electrode process water and 1'339 mg/l for the negative electrode process water. These values are in good agreement with the results obtained from ICP-OES analysis (compare Table 1).

In conclusion, the lithium concentrations particularly in the negative electrode process water are comparable to or even exceed those found in typical commercial primary lithium brines where concentrations typically range between 200 and 1'400 mg/l [13]. To assess the accumulation of metallic elements during the recycling process, two samples were collected from the positive electrode (i.e., Positive electrode PW- 26kg and 90 kg) and the results from both ICP-OES and NMR clearly demonstrate a substantial

increase in the concentrations of lithium, iron and aluminium in the process water- by a factor of three to five – by the end of the process.

As discussed above, the copper concentrations exceed the permissible disposal concentration of 1 mg/l. The other elements do not have specified threshold values for discharge into water bodies [10]. However, the high lithium concentration in process water highlights its potential as a valuable secondary source of lithium. Identifying this opportunity, a preliminary study with the University of Applied Sciences and Arts Northwestern Switzerland (FHNW) will be dedicated to recover lithium through membrane-based separation techniques. Technologies such as nanofiltration and reverse osmosis potentially enable selective and effective lithium extraction. In parallel, for example copper, along with other impurities remain in the retentate, simplifying its disposal. During the development of this process, additional pre-treatment procedures for the water samples will be investigated, including pH adjustment and removal of suspended particles. A proposal for additional funding regarding this work has been submitted to Inno-Cheque (Application Number: 76609.1 INNO-EE) with the goal to recover the lithium.

Air quality

In previous measurements at an earlier stage of the project, traces of airborne graphite along with carbon black were reported (see Appendix 7.2). The maximum exposures of this carbon black like species were 6.93 x 10^{-2} µg/m^3 inside the LIBERTY 1.0 machine. This maximum concentration was below the permissible limit of 3.5 mg/m^3 defined by the Occupational Safety and Health Administration. The same tests were repeated upon installation of the latest reactors and separation unit as also potential traces of carbon nano tubes (CNT) and other potential respirable dusts should be identified. All measurements were carried out by Gruner AG and were based on SEM/EDX analysis and Raman Spectroscopy. The results of the measurements were then compared to the maximum allowable concentration (MAC) according to the standards of the Swiss Accident Insurance Fund (SUVA) [14]. The measurements were performed at the following positions:

- At the reception/entrance
- In the kitchen, across from the recycling facility
- Outside (next to) the LIBERTY 1.0 machine
- Inside the LIBERTY 1.0 machine

The results of these measurements are summarized in Table 3. It was found that all measured species were well below the MACs and the reference values from Suva limits. Respirable dust, i.e. "E-Dust" (particles so small that that they can be absorbed through the respiratory tract when inhaled), showed concentrations below detection limits. The same applied for CNTs in these measurements. Traces of lithium (7 - 14 µg/m³) and copper (0.6 - 1.8 µg/m³) were found but were one to two orders of magnitudes lower than the MAC [14].

Table 3: Results of air quality measurements at different locations of the recycling facility. Values with "<" represent results below the detection limits of the applied method. The concentrations for E-Dust and CNTs were below detection limits.

Location	Duration [min]	"E-Dust" [mg/m³]	Lithium [µg/m³]	Copper [µg/m³]	CNT [fibers/m³]
At the reception/entrance	194	<0.10	7	0.6	<9'900
In the kitchen	191	<0.10	7	0.6	<9'900
Outside (next to) LIBERTY 1.0	174	<0.11	8	0.7	<9'900
Inside LIBERTY 1.0	92	<0.21	14	1.8	<9'900
MAC-value over 8h daily		*10*	*200*	*100*	
	Reference value according to Suva limit value list				*10'000*

Further measurements to assess the air quality were performed aiming at volatile organic compounds (VOC). The measurements were performed at the following positions:

- Inside the LIBERTY 1.0 machine without activated carbon filter
- Inside the LIBERTY 1.0 machine with an activated carbon filter
- In KYBURZ' laboratory inside the fume hood
- In KYBURZ' laboratory outside the fume hood

The highest value was measured inside the LIBERTY 1.0 machine before the installed filter system with 31'700 µg/m³ total sum of all VOC (TVOC). This exposure could be explained with the loss of volatile electrolyte solvents during disassembly of cells (compare section 2.1.1).

For all substances with concentrations higher than > 100 µg/m³, the according MAC values were on average about 1'000 times larger than the measured values (not shown). This suggests that no further measures are mandated. Nevertheless, respiratory protection (Dräger X-plore 8000 A2 P R SL) for staff was implemented as part of KYBURZ' occupational safety policy.

Furthermore, after installing an activated carbon filter to process all air from the facility and laboratory, this TVOC value was further reduced by about 50 %. It seems possible to reduce the remaining TVOC value even further by optimizing the filter system accordingly. Measurements on lab-scale showed a reduction potential of up to 99%.

Outside the LIBERTY 1.0 facility, the concentrations were drastically lower compared to inside the facility. Assuming that all found contaminations stem from the recycling operation, this proves that the current system to be 95 % effective.

2.1.5. Economic potential and competitiveness

To assess the economic viability of battery recycling processes, it is necessary to consider not only the associated costs but also the potential revenues generated by the respective technologies. For conventional, hydrometallurgy-based recycling approaches, the value chain can be roughly broken down as follows. The main cost elements along the value chain are:

1. Collection and transport: 10–15%
2. Pre-processing (e.g. analysis and dismantling): 10–15%
3. Black mass production (shredding) and transport to the offtaker (Asia): 30–40%
4. Metal extraction (e.g. via hydrometallurgy): 30–40%

In the case of black mass production, a further breakdown can be made into:

1. Process-related costs
2. Overheads and capital expenditure
3. Fixed costs

Actual cost structures vary from plant to plant and operator to operator and are generally considered confidential business information. Estimates differ significantly across sources. Figure 8 shows indicative values for the recycling of LFP batteries and compares different process routes [15]. The costs for direct recycling are lower in comparison to conventional processes, while the expected LiFePO4 revenue of direct recycling exceeds the material revenue from the conventional processes.

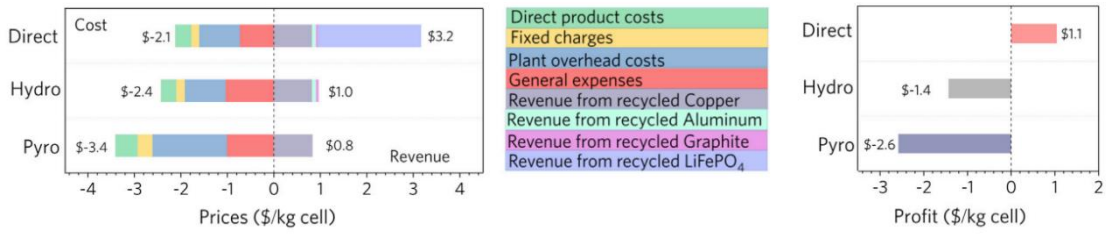

Figure 8: Indicative values for the recycling of LFP batteries comparing different process routes [15].

While costs depend only to a limited extent on the specific battery chemistry being processed, there are substantial differences on the revenue side depending on the cell type.

The intrinsic material value of nickel-based chemistries is estimated depending on source and market conditions at approximately USD 10 per kg or USD 40 per kWh. By contrast, nickel- and cobalt-free chemistries such as LFP have significantly lower intrinsic values, in some cases up to 50% lower.

This results in several current challenges for battery recyclers in Europe:

1. Existing and planned facilities for black mass production involve high capital expenditures, regardless of actual utilization. At the same time, the volume of end-of-life batteries remains below expectations from recent years. This leads to elevated unit costs per tonne of processed material.
2. The limited availability of refining capacity within Europe means that black mass must largely be shipped to Asia primarily to China and South Korea incurring additional logistics costs of several hundred CHF per tonne. These costs are typically borne by the exporter, i.e. the recycler.
   Furthermore, as of 9 November 2026, an amendment to the EU Waste Shipment Regulation

will classify black mass as hazardous waste, making its export to non-OECD countries such as China strictly prohibited. Even exports to OECD countries like South Korea will become significantly more difficult, due to expanded documentation requirements, permitting procedures, and return obligations. As a result, many European recyclers will not only lose access to a key market but will also face growing structural pressure to establish domestic refining capacities or to develop alternative recycling pathways that are both legally compliant and economically viable within Europe [16], [17], [18].

3. The current market situation is characterized not only by a global oversupply of cells but also by overcapacities across the upstream segments of the battery value chain. This places downward pressure on the prices of virtually all materials used in battery production. Current market prices for these materials are in some cases more than 80% below their 2022/2023 levels.
4. As a consequence of point 3 and the slower-than-expected ramp-up of electromobility particularly in Europe and North America many investments in battery production capacity and upstream value creation across Europe are either delayed or cancelled altogether. This deprives recyclers of further access to high-value material streams required for stable operations.

These challenges are reflected in the difficulties currently faced by recycling companies, culminating in the recent insolvency proceedings filed by Li-Cycle, one of the largest and most well-known battery recyclers in North America and Europe [19].

It is therefore evident that the lithium-ion battery recycling business model is reaching its limits under current conditions or will in the foreseeable future remain dependent on cross-financing schemes, such as those in place in Switzerland under the VEG framework.

Should LFP and other low-value chemistries such as the increasingly discussed sodium-ion batteries gain further market share, the pressure on conventional battery recycling models will intensify.

A possible way forward is offered by the direct recycling process developed by KYBURZ. This approach not only aims to reduce process costs to a target level below 1'500 CHF per tonne, but also significantly lowers transport and capital expenditures through its decentralised, small-scale plant design.

If the European lithium-ion battery industry stabilises and that a corresponding value chain becomes established, the achievable revenues could also increase substantially. If sufficient volumes and material quality are reached, sales prices of CHF 2 - 5 per kg of LFP recyclate (equivalent to approx. 0.80 - 2.00 CHF per kg of cell mass) may become attainable. This would for the first time create a scenario in which material revenues from LFP batteries could exceed the pure processing costs.

2.2 Output-related aspects

2.2.1. Metal fractions

The different metallic output fractions can be introduced back into the material value streams through established recycling processes. The value of these materials is dependent on three major factors: the material price (London metal exchange, LME), the material quality and the material quantity. The imbursement for the materials is individually negotiated based on the LME material price and applicable deductions for quality (i.e. level of impurities or form, for instance foils and wires versus "dense" materials) and quantities (typically for anything smaller than 5 tonnes per shipment). Currently (April 2025) on LME aluminium is traded for around 2'500 $/t. Copper is traded at around 9'000 $/t. For quantities smaller than 5 tonnes, deductions down to 12.5 % of the original prices are possible. For these small quantities local waste management companies must be involved which have to collect, handle and transport the materials, whereas large quantities can be shipped to smelters directly. To illustrate the mechanism, Table 4 shows the realistic values for certain combinations of materials and qualities. The highest price can be achieved for dense metal parts that are offered at quantities over 5 tonnes. The copper prices outweigh the aluminium prices significantly.

Table 4: Material prices for metal fractions with respect to their condition. The highest price can be achieved for dense metal parts at high quantities. Copper prices are higher than aluminium prices.

Material	**Base price**	**Quality**		**Quantity**	
		State	Purity	< 100 kg	> 5'000 kg
Copper	9 $/kg	Foil	80 %	2 $/kg	5 $/kg
		Dense	95 %	5 $/kg	8.5 $/kg
Aluminium	2.5 $/kg	Foil	96 %	0.05 $/kg	0.4 $/kg
		Dense	98 %	1.5 $/kg	2 $/kg

As described in Figure 6 the recycling process produces different metallic output fractions, which are either aluminium or copper metal parts. Table 5 summarizes the different metallic fractions with their masses and shares. The highest share by mass is the copper current collector foils with approximately 53 %. The dense metal pieces from the connector tabs make up the lowest shares with combined 22 %. According to the material values given in Table 4, hypothetical material revenue scenarios were estimated for KYBURZ' metal outputs of one single 180 Ah cell in Table 5.

Table 5: Masses and shares of the different metal output fractions per one 180 Ah cell. Based on metal prices, a minimum and maximum revenue scenario could be estimated. The present situation of the recycling process corresponds to the minimum scenario, where the recovered current collectors are foils and quantities below 100 kg. When storing the metals until quantities of more than 5 tons are achieved and the current collector foils get pressed to metal blocks, a maximum revenue scenario results. The revenue could potentially be increased from 1.92 $/cell up to 6.43 $/cell.

Metal output fraction	**Mass [g]**	**Estimated revenue [$]**		
		min. scenario	max. scenario	difference
Aluminium tabs	70 (7 %)	0.11 (6 %)	0.14 (2 %)	0.03
Copper tabs	148 (15 %)	0.74 (38 %)	1.26 (20 %)	0.52
Aluminium current collector	254 (25 %)	0.01 (1 %)	0.51 (8 %)	0.5
Copper current collector	532 (53 %)	1.06 (55 %)	4.52 (70 %)	3.46
TOTAL	*1'004 (100 %)*	*1.92 (100 %)*	*6.43 (100 %)*	*4.51*

The current situation, in which materials are processed in their "as-collected" state, represents the minimum revenue scenario. The current collectors were recovered as foils at quantities below 100 kg. According to the metal prices, a revenue of 1.92 $/cell could be estimated for the metal output fractions in the as collected state. In this scenario, copper contributes 93 % of the total revenue. To increase the revenue from the metal output fractions, KYBURZ has two options. First, the metals can be collected over many recycling batches until the quantities of the collected metal output fractions exceed 5 tons. Second, the collected current collector foils could be pressed to dense metal blocks. Both options lead to higher material prices which are estimated in the maximum revenue scenario. The difference between the two scenarios is significant as the revenue could be increased by 4.51 $/cell. This corresponds to a revenue gain of 335 %.

2.2.2. Positive electrode active layer material ($FePO_4/LiFePO_4$)

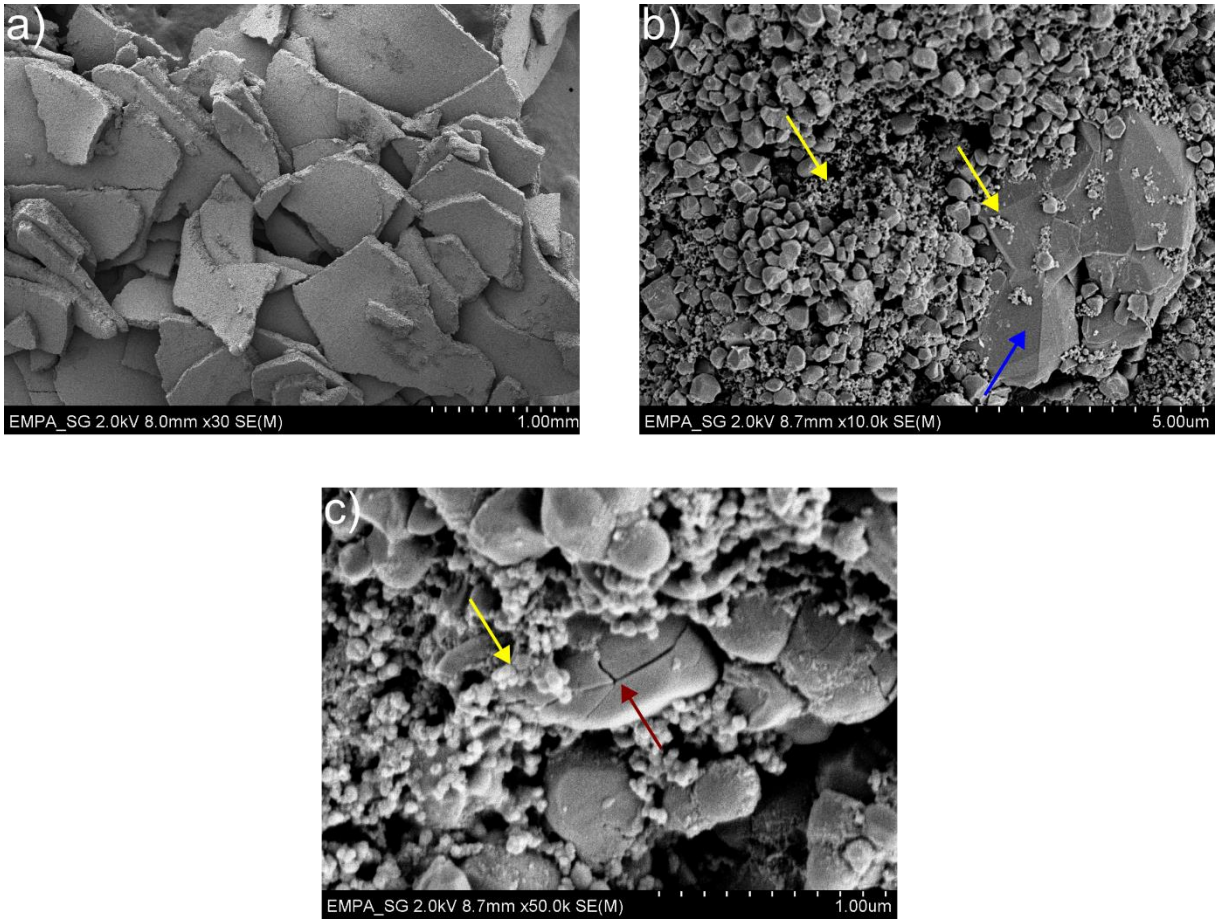

Figure 9: Images of the active layer material in the "as collected" state. a) Overview of the material in the SEM showing flakes of the delaminated active layers, b) detail of the aggregates of $FePO_4/LiFePO_4$ active material particles in the harvested material with carbon black particles (yellow arrows) and an embedded graphite particle (blue arrow), c) high magnification image of an $FePO_4/LiFePO_4$ active material particle that shows an active material particle with a crack (red arrow).

As described in section 2.1.2 the active layer coating was collected as flakes where the cohesion within the layer was mostly intact (see Figure 9 a). This means that the active layer material still needs to be considered as the composite that was produced during production. Thermogravimetric analysis suggested that the composite was probably held together by a carboxy methyl cellulose (CMC) based binder system. CMC is a known aqueous binder and was quantified to contribute around 3.5 % wt in the output material (not shown).

The microstructure reveals the other components in this output material. Besides the $FePO_4/LiFePO_4$ active material particles which make up most of the microstructure, graphite particles (blue arrow) and carbon black (yellow arrows) were found as shown in Figure 9 b. Both carbonous materials were expected to be added during manufacturing as a conductive additive to decrease the internal resistance of the positive electrode coating and therefore cell. On the one hand, it could be seen as an impurity in the recovered $FePO_4/LiFePO_4$ material. On the other hand, it does not need to be added during the production of new cells, which is environmentally beneficial as it reduces the demand for further carbonous primary materials. On a selective detail image, a cracked active material particle could be observed (red arrow in Figure 9 c) which might also come from ageing of the material during the use phase. However, most of the particles observed in the SEM were morphologically intact.

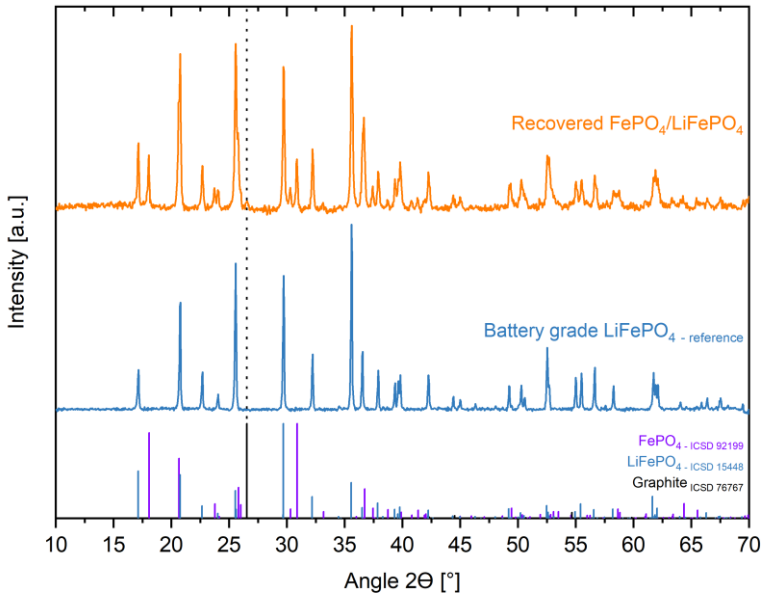

Figure 10: X-ray diffractogram of the recovered $FePO_4/LiFePO_4$ active material in comparison to battery grade $LiFePO_4$ reference material. The recovered material consists of two phases that correspond to $LiFePO_4$ and its delithiated $FePO_4$ counterpart. Also, graphite could be identified (black dotted line).

The recovered $FePO_4/LiFePO_4$ material after processing 90 kg of electrodes was analysed with X-ray diffraction (XRD) and compared to battery grade reference material (see Figure 10). In the recovered material three different crystallographic phases were identified: orthorhombic $LiFePO_4$ and its delithiated but also orthorhombic counterpart $FePO_4$. As already seen in the SEM, the crystalline graphite could be identified with the reflection around 26 ° two theta (black dotted line in Figure 10). Before disassembly, the cell was discharged to 2 V which means that the lithium should be completely intercalated back into the $LiFePO_4$ active material. Yet, there is still delithiated $FePO_4$ remaining. As no crystalline side phases could be observed, the main ageing mechanism of the material could be ascribed to loss of lithium inventory during battery use. A potential route for relithiation of the remaining $FePO_4$ was investigated according to literature [20] and is topic of a research paper in preparation.

A phase quantification of final output after processing 90 kg of electrodes showed that the samples consisted of 72.5 % $LiFePO_4$, 26.8 % $FePO_4$ and 0.7 % graphite. The $FePO_4/LiFePO_4$ ratio after processing 90 kg of electrodes aligns with the results of the previous material quality study (see Appendix 7.3) where it was found that independent of the SoH, the fractions of the two phases were approximately constant around 27 % $FePO_4$ and 73 % $LiFePO_4$. However, the reflection of the graphite in the recovered $FePO_4/LiFePO_4$ (follow black dotted line in Figure 10) is notably smaller in comparison to the previous study. Indeed, the graphite content was reduced from ca. 7 % to 0.7 %. This might be explained by the presence of carbon black in the later output products that compensate for the reduced graphite content. Carbon black was hardly detectable by XRD as it is not crystalline. Potential reflections from disordered graphitic planes were expected to be dominated by $LiFePO_4$ peaks and hence won't be visible [21], [22].

For the recovered $FePO_4/LiFePO_4$ it was shown that the material achieves only around 70 % of the discharge capacity of primary battery grade $LiFePO_4$ (see Appendix 7.4). However, a potential customer showed that when adding 10 % wt of the recovered $FePO_4/LiFePO_4$ to the production of primary $LiFePO_4$ material, the discharge capacity could be increased by 6 - 7 % in comparison to their primary $LiFePO_4$ only (results not shown). This test has been carried out internally by the potential customer and the result might be explained by using a half-cell setup (i.e. $FePO_4/LiFePO_4$ vs. lithium metal), where the $FePO_4$ could be relithiated electrochemically.

In conclusion, the recovered output material from the positive electrode is expected to consist of mixtures of $FePO_4/LiFePO_4$, graphite, carbon black and binder. However, as all cells are discharged to the same voltage and the $FePO_4/LiFePO_4$ ratio was shown to be independent of the SoH, the "quality" of

the active material itself is not expected to be affected. Moreover, there is a market interest on KYBURZ' secondary $FePO_4$/$LiFePO_4$ output material as a potential customer was found who can feed the recovered material in the production of their pristine $LiFePO_4$ material.

As for the economic potential of the recovered $FePO_4$/$LiFePO_4$ material it has to be noted, that currently the overall lithium-ion battery value chain does not exist in a mature enough state in Europe, such that larger quantities, exceeding the need for research purposes, cannot be sold right now, despite a theoretical value of 2 - 5 €/kg, depending on Li-content and process route. It is expected that by the end of the decade this bottleneck will be overcome, and the recovered $FePO_4$/$LiFePO_4$ material can be sold to off-takers in relevant quantities and at reasonable prices, which will massively contribute to the economic potential of the entire LFP-battery recycling.

2.2.3. Negative electrode active layer material (graphite)

The collected graphite active layer material had a dryness of ca. 70 % after the separation from the process water. The residual moisture in the semi-dried graphite is not considered a disadvantage. Instead, it suppresses dust formation and thus simplifies storage and transport of the material. Moreover, the materials properties are not expected to be negatively impacted by the residual humidity.

Figure 11 shows the material in the "as-collected" state. The macroscopic photograph shows the graphite active layer material collected as nuggets of various sizes (Figure 11 a). The visual investigation in the SEM showed that the nuggets consisted of graphite particle aggregates (Figure 11 b - c). These particle aggregates were considered as composites because the individual graphite particles were hold together by remaining binder from the original active layer coating. Moreover, carbon black originating from cell manufacturing was still present on the graphite particle surface as shown in the detail Figure 11 d (yellow arrows). Finally, more artefacts that could originate from battery ageing or the recycling process like minor metallic impurities could be observed locally at high magnifications (not shown). Disregarding this minor and localized artefacts, the harvested active layer material consists of carbon which was confirmed in EDX as no other elements could be observed in representative measurements.

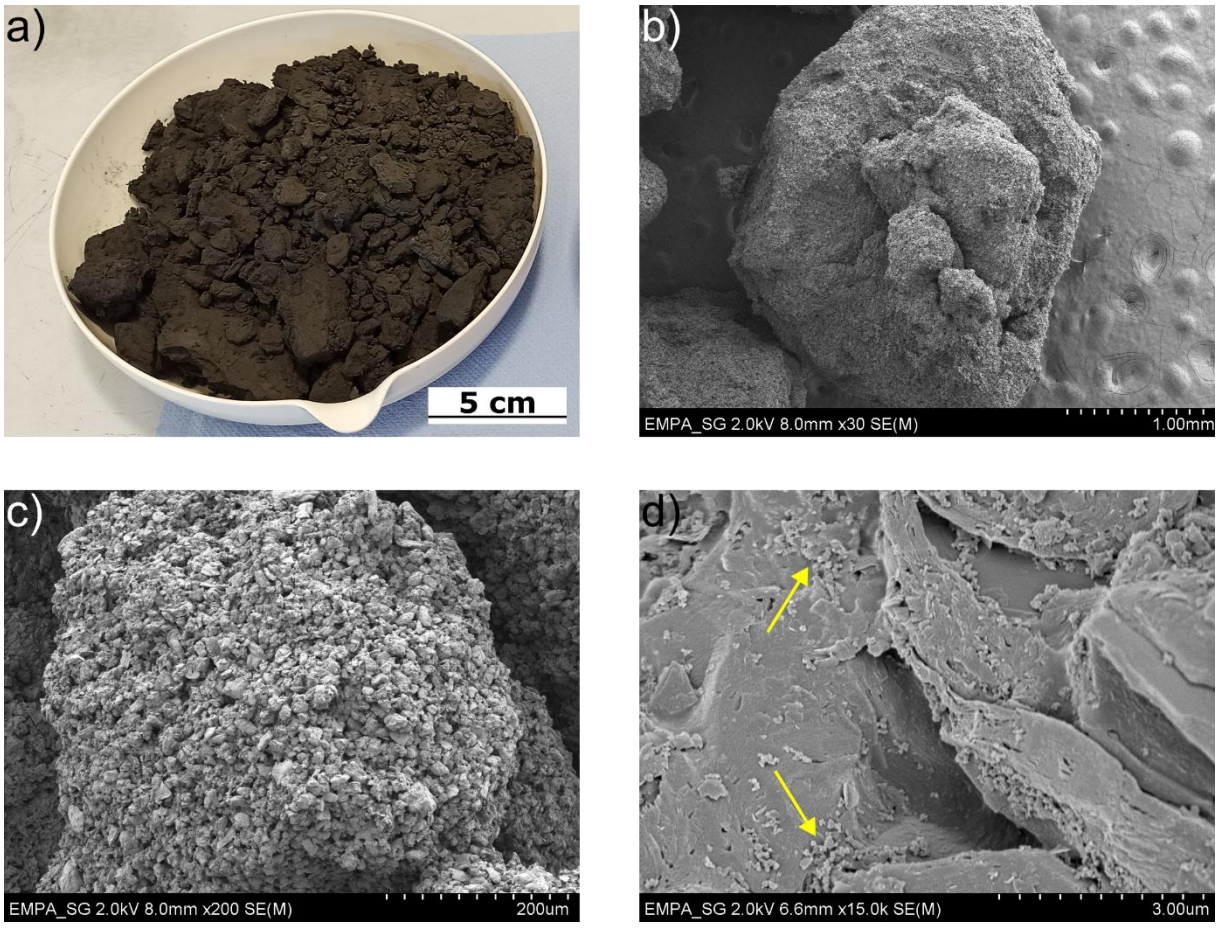

Figure 11: Images of the active layer composite in the "as collected" state after the separation unit. a) Macroscopic photograph of the material after drying, b) overview of the material in the SEM, c) aggregates of the graphite active material particles in the harvested material, d) carbon black particles are visible on the surface of the graphite particles (yellow arrows).

To identify potential negative impacts of the separation unit on the material quality, the graphite was compared before and after its separation of the process water. For this, sedimented material from the tank was analyzed with SEM/EDX and XRD and compared with recovered material after the separation unit. Indeed, more surface artefacts were found on the sedimented material. For example, more binder residues, electrolyte salt components and metallic components were discovered in SEM/EDX (not shown). This was also confirmed by XRD measurements as shown in Figure 12. Indicated with the black arrows, more crystalline artefacts could be measured on the material before the separation unit. The specific crystalline phases of the artefacts could not be identified as they consisted of various chemical compositions containing copper, aluminium and fluoride. Also, oxygen containing artefacts could be observed with EDX in the sedimented material. These artefacts are expected to come from the cellulose binder. As less artefacts could be observed in the material after the separation from the process water, the material quality improves when collected after the separation unit.

The hypothesis for this quality difference is that the separation unit removes most of the water from the sample. As the impurities described above are expected to be dissolved and dispersed in the process water they could condense on the surface of the material when it is not removed. Hence, reducing the process water content in the material leads to less artefacts as the material after the separation unit shows less artefacts in comparison to the material collected from the sediment in the tank.

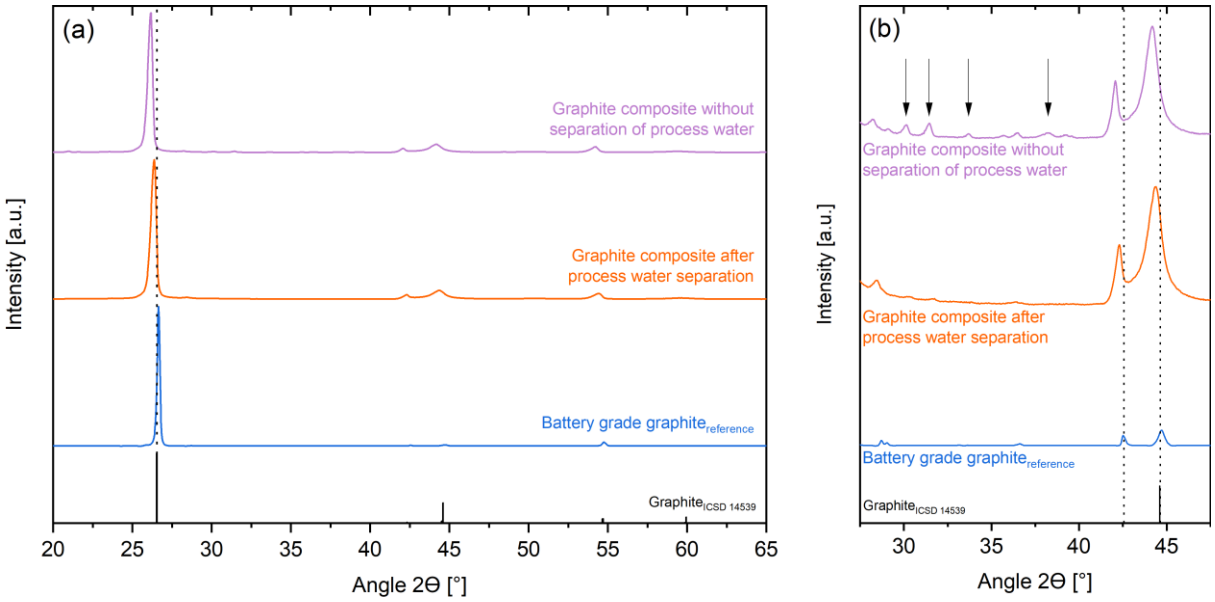

Figure 12: X-ray diffractograms of recovered graphite active material in comparison to battery grade graphite as a reference. a) X-ray diffraction pattern from 20 to 65 degrees 2theta with the strong diffraction originating from the interlayer spacing between the graphene layers of the graphite around 26 °. b) Zoom in of the patterns indicating crystalline artefacts in the harvested active layer composite (black arrows).

When comparing the X-ray diffractograms of the recovered graphites with battery grade reference graphite the reflection around 26 ° shifted towards lower angles for the recovered graphite (see Figure 12). According to Bragg's law this indicates an increase in the lattice spacing of the crystal structure. Since this reflection originates from the interplanar spacing of the graphene layers, the shift could originate from remaining lithium that was still intercalated in the graphite because intercalated lithium pushes the graphene layers apart [23]. This could be supported by the observable peak broadening which could indicate microstrain in the lattice due to the remaining lithium intercalation and the resulting volume expansion. Although, peak broadening could also arise from smaller crystallite size due to ageing phenomena.

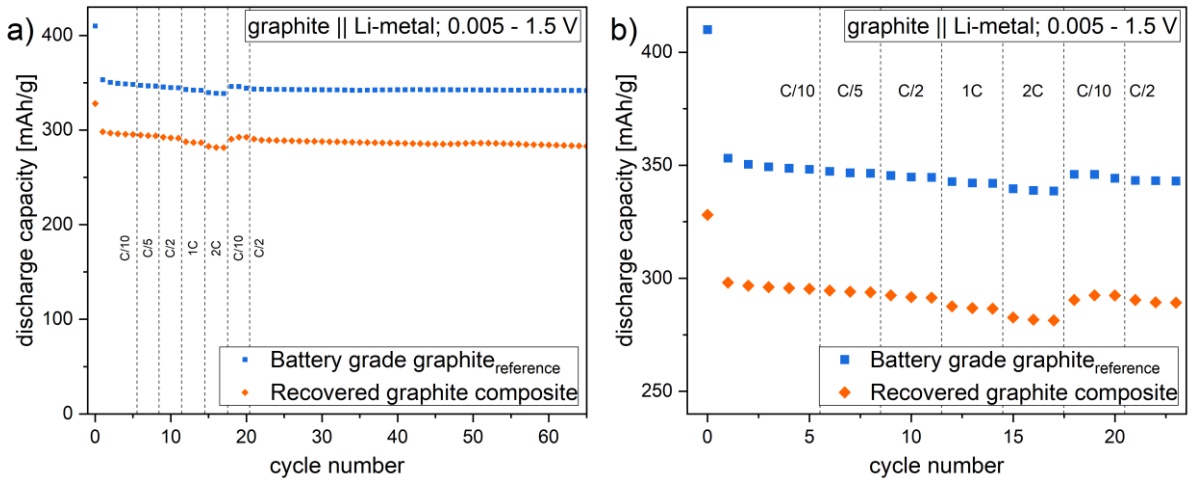

Figure 13: Discharge capacities of graphite half-cells at different C-rates. a) Comparison between pristine battery grade graphite as a reference material and the recovered graphite composite, b) shows a

more detailed overview of the rate performances of the two materials. The rate performances of the recovered graphite are ca. 50 mAh/g lower in comparison to the pristine battery grade graphite.

The recovered graphite material was electrochemically tested on its discharge capacities in comparison to fresh battery grade graphite material available on the market as a reference (see Figure 13). It was shown that the discharge capacities of the recovered material were constantly around 50 mAh/g lower in comparison to the reference material. This corresponds to 85 % of the discharge capacity of primary battery grade graphite. Both materials follow the same pattern when varying the C-rates as shown in the detail Figure 13 b. Potential explanations for the lower discharge capacities might be the degradation of the material during its use phase and a potential impact of the recycling process. Both might lead to the artefacts found in the XRD analysis which could be detrimental to the dis-/charging behaviour.

To investigate a suitable method to remove artefacts from recovered graphite material a research paper is in preparation. The goal of this paper is to remove the artefacts of graphite and show their influence on the crystallographic and electrochemical properties. So far it was found that the artefacts could be removed. However, experience also shows a very fast material development of graphite active materials. For example, there are different trends for the use of graphite in cells regarding particle sizes, morphologies, presence of carbon black and crystallite sizes. Moreover, the graphite could originate from natural or synthetic sources. Even if two cells from the same producers with the same specifications but different generations are opened, the graphite will most likely be different. Applying this to recycling, where a random mixture of different cells (specifications, generations and suppliers) will be processed, the recovered graphite material will also be a random mixture of graphites. Hence, it is questionable whether this material will end up in new batteries, even when the material properties could be restored. Although graphite is not yet subject to recycled content requirements under the EU battery regulation it is already included in the due diligence obligations of the regulation and the production of secondary graphite is seen as environmentally favourable as it reduces the demand of primary graphite. Potential other applications apart from batteries are therefore currently being investigated.

In conclusion, the recovered material from the negative electrode is expected to consist of mixtures of different graphite active materials when treating different cells. It was shown that the separation unit positively impacts the material quality as less artefacts could be found on the material after process water separation. Some minor and localized artefacts could be observed, though, but the recovered active layer composite consists mostly of graphite. Its discharge capacity reaches only approx. 85 % in comparison to pristine battery grade graphite. Hence, it is questionable whether the material will be reused for battery applications. However, other potential applications for the use of this secondary graphite are under investigation.

The economic potential of recycled graphite highly depends on the later use. As with the recovered $FePO_4$/$LiFePO_4$ material unfortunately right now the value chain for the production of lithium-ion batteries in Europe is in an immature state, such that for the time being no off-take-agreement for larger quantities, exceeding lab-scale, can be closed, limiting the economic potential of the recycling operation for the time being. Again, it is expected that by the end of the decade, with the development of a battery-production value chain in Europe, this bottleneck can be overcome.

2.2.4. Recovery of materials

The EU battery regulation defines rates of recovery for selected materials from lithium-based batteries. The target materials in the present case are copper and lithium which are described in detail in the following subchapters. For the calculation of the rate of recovery of materials the following formula is defined:

$$rRM(TM) = \frac{\sum m_{TM,output-point}}{m_{TM,input}} \times 100, [mass\ \%]$$

where:

TM = target materials (copper and lithium) according to Part C of Annex XII in the regulation,

rRM = calculated rate of recovery of materials from waste batteries in relation to recycling [mass %],

$m_{TM, output\text{-}point}$ = mass of the target material in output fractions considered in the rate of recovery of materials per calendar year [in tonnes],

$m_{TM, input}$ = mass of the target material in the input fraction per calendar year [in tonnes].

The ambitious targets for recovery of materials are shown in Table 6 and will stepwise be increased with time.

Table 6: Targets for recovery of materials according to the EU battery regulation. The targets are stepwise increased with time.

Material	≥ 31.12.2027	≥ 31.12.2031
Copper	90 %	95 %
Lithium	50 %	80 %

Because KYBURZ' recycling facility is still in pilot phase, the mass is just considered as the mass of a single 180 Ah cell in grams and not in tons per calendar year. This simplification should not affect the calculation of the recycling efficiency because the input and output masses are expected to scale linearly by the same factor when extrapolating to a full calendar year.

Rate of copper recovery

Copper can be recovered from two sources in the recycling process. First from connector tabs at the cell casing and second from the recovered current collector foils of the negative electrodes.

Since the connector tabs could manually be unscrewed from the cell casing without damaging them, they could be completely recovered. KYBURZ expects that this process step can easily be automatized.

During recovery of the copper current collector foils in the delamination of the negative electrodes, no visual loss or destruction of the copper foils was observable (compare section 2.1.2). The process water of the delamination process showed 8.93 ppm of copper contamination (compare 2.1.4). And in SEM/EDX analysis of the recovered graphite some copper could selectively be identified at high magnifications (not shown). However, in contrast to the recovered copper foil mass of 532 g/cell these artefacts are considered as trace losses. Hence, all copper originating from the negative electrodes was considered as recovered.

To conclude, all the copper from the cell could be collected and the copper output fraction $m_{Cu, output}$ is equal to the input fraction of copper $m_{Cu, input}$, which results in a rate of copper recovery of rRM(Cu) = 100 %. The rate for copper recovery therefore already exceeds the 95 % demanded by latest end of 2031.

Rate of lithium recovery

To calculate the rate of lithium recovery the output mass and the input mass of lithium must be estimated. For these estimations the following assumptions were made.

The only lithium containing output fraction of the recycling process is the $FePO_4$/$LiFePO_4$ active material from the positive electrode. $m_{Li, output}$ is calculated based on the ratio of the molar masses of lithium in $LiFePO_4$. As described in section 2.2.2 the output fraction contained 3.5 % binder and of the recovered active material only 72.5 % was $LiFePO_4$. Hence, the mass of the lithium output translates to

$$m_{Li,\ output} = \frac{M_{Li}}{M_{LiFePO_4}} \times m_{LiFePO_4} = \frac{M_{Li}}{M_{LiFePO_4}} \times 0.725 \times 0.965 \times m_{HM+\_dry}$$
$$= \frac{6.94\ \frac{g}{mol}}{157.76\ \frac{g}{mol}} \times 0.699 \times 1'733\ g = 53.35\ g$$

For the calculation of the lithium content in the input fraction $m_{Li,\ input}$ more assumptions need to be made. Lithium sources in the cell are the molar fractions of the $LiFePO_4$ active material and the electrolyte salt:

$$m_{Li,\ input} = \frac{M_{Li}}{M_{LiFePO_4}} \times m_{LiFePO_4,\ input} + \frac{M_{Li}}{M_{LiPF_6}} \times m_{LiPF_6,\ input}$$

where $m_{LiFePO4,\ input}$ consists of the recovered active material (m_{HM+_dry}) and the active material that was lost during production of the output material ($\Delta m_{delamination}$) considering the binder content of 3.5 %. And for $m_{LiPF6,\ input}$ it was assumed that the electrolyte was 1 M LiPF6 in EC/EMC (3:7 by weight) which is a commonly used electrolyte for high power applications. Further, it was assumed that the electrolyte mass corresponds to $\Delta m_{disassembly}$ = 170 g that were attributed to be the loss of the volatile electrolyte solvent (compare section 2.1.1). This might be an underestimation as some electrolyte could also remain in the separator and the electrode foils. However, it is expected that it results in the right order of magnitude. Moreover, as shown below, the lithium mass from the electrolyte contributes only a minor fraction to the total lithium mass in the cell. Hence, the mass of the lithium input translates to

$$m_{Li,\ input} = \frac{M_{Li}}{M_{LiFePO_4}} \times 0.965 \times (m_{HM+_{dry}} + \Delta m_{delamination}) + \frac{M_{Li}}{M_{LiPF_6}} \times c \times M_{LiPF6} \times V_{electrolyte}$$
$$= \frac{M_{Li}}{M_{LiFePO_4}} \times 0.965 \times (m_{HM+_{dry}} + \Delta m_{delamination}) + M_{Li} \times c \times \frac{\Delta m_{disassembly}}{\rho_{electrolyte}}$$
$$= \frac{6.94\ \frac{g}{mol}}{157.76\ \frac{g}{mol}} \times 0.965 \times (1'733\ g + 98\ g) + 6.94\ \frac{g}{mol} \times 1\ \frac{mol}{l} \times \frac{170\ g}{1098\ \frac{g}{l}}$$
$$= 77.7\ g + 1.07\ g = 78.77\ g$$

According to this calculation the lithium input mass from $LiFePO_4$ active material contributes 98.6 % to the total lithium input mass and only a minor contribution comes from the electrolyte with 1.4 %.

Finally, the rate for recovery of lithium is

$$rRM\ (Li) = \frac{m_{Li,\ output}}{m_{Li,\ input}} \times 100\ \% = \frac{53.35\ g}{78.77\ g} \times 100\ \% = 67.7\ \%$$

When comparing the resulting rRM(Li) with the 50 % target from the regulation the KYBURZ process is already reaching this aim, almost three years before the mandatory deadline. However, by the end of 2031 80 % recovery of lithium must be achieved. Especially the anode water shows high lithium concentrations comparable to lithium brines for primary lithium production (compare section 2.1.4). Currently, KYBURZ in collaboration with FHNW - School of Life Sciences has applied for funding for a feasibility study (Inno-Cheque) on using the process water as another source for lithium recovery.

2.2.5. Other material fractions

As described in section 2.1.3 not all the recovered materials can be considered as output fractions according to the EU battery regulation. The non-accountable output materials are plastic fractions that need to be incinerated. For example, the cell housing is not allowed for recycling as it consists of brominated polymers acting as flame retardants [24]. Thus, they must be incinerated. The total mass of the plastic fraction $m_{Plastics}$ (1'410 g) accounts to 25.6 % of the cell mass (5'500 g) and makes up 27.5 % of the mass of the recovered materials. The different components of the plastic output materials are summarized in Table 7.

Table 7: Components of the plastic material fractions with their masses in grams and relative shares in %. The biggest mass contribution comes from cell housing.

Material fraction	Mass [g]	Share [%]
Housing + Lid	735 + 155	63
Wraps of electrode stack	25	2
Separator	495	35
TOTAL	*1'410*	*100*

The cell housing contributes 63 % to the total mass of plastic output materials. Cells of later generations show a clear trend towards metal casings. Since metal casings can be recycled in conventional metal recycling routes, the overall recycling efficiency of KYBURZ' direct battery recycling process will significantly be increased because the casing will then be accountable as an output fraction according to the regulation.

2.3 Life cycle assessment

A Life Cycle Assessment (LCA) study has been conducted in order to evaluate the environmental performance of the direct recycling process for LFP battery cells, developed by KYBURZ. The main objective of this LCA study is to identify the ecological hotspots, i.e., the environmentally most impactful process steps within this recycling process, and to assess the carbon footprint associated with each of the steps.

The study uses a standardized LCA approach to quantify the environmental burdens of the examined processes. Specifically, the LCA adheres to the guidelines of ISO 14040 and ISO 14044 [25], [26], which structure the analysis in four key phases:

1. Definition of goal, scope, and functional unit
2. Compilation of a life cycle inventory (LCI)
3. Impact assessment using selected environmental indicators
4. Interpretation of results

Table 8 summarizes the key elements of the present study in relation to these four phases.

Table 8: Overview of methodological choices in the LCA study.

LCA Phase	Information
I – Goal & Scope	• Evaluate the environmental footprint of KYBURZ' direct recycling process • Identify potential hotspots • Functional unit: 1 kg of EoL LFP battery cell treated with KYBURZ' direct recycling process
II – Inventory Analysis	• System boundaries: from EoL LFP cells to marketable output materials (i.e. to materials that can be sold to third parties) • Foreground: primary data from KYBURZ • Background: ecoinvent 3.9.1 [27] • Software: Brightway2 via Activity Browser interface [28]
III – Impact Assessment	• Environmental Footprint (EF) 3.0 no long term effects (European Commission Joint Research Center (JRC)) [29] • Umweltbelastungspunkte (UBP) total [30]
IV – Interpretation	• Comparative analysis of different scenarios • Identification of key contributors to total environmental impact

The geographical boundaries of the study are limited to Switzerland, where the entire recycling process takes place. The functional unit is defined as 1 kg of EoL LFP battery cells entering the direct recycling process performed at KYBURZ – a usual way of defining the functional unit when evaluating end-of-life processes. Focusing on the end-of-life processes, the production of the LFP batteries are excluded from the examination, meaning that environmental impacts associated with raw material extraction and battery manufacturing are excluded from the here examined system. The system boundaries are covering the entire KYBURZ recycling process and therefore consist of the following process steps:

- Discharging of EoL cells
- Disassembly of cells and unwinding with semi-automated machine (LIBERTY 1.0) to remove housing, tabs and to separate electrodes from the separator
- Waste treatment of residual fractions (e.g., plastic)
- Delamination of electrode foils in the reactors
- Packing and transporting aluminium and copper to external recyclers
- Recovery of $FePO_4$/$LiFePO_4$ flakes using a buffer tank for sedimentation
- Graphite dewatering via process water separation
- Transportation of semi-dried graphite and $FePO_4$/$LiFePO_4$ flakes

KYBURZ' direct battery recycling process for a 5.5 kg battery cell is described in more details in paragraph 2.1 and illustrated in Figure 12, which shows the entire recycling chain for the treatment of LFP cells considered in this LCA analysis.

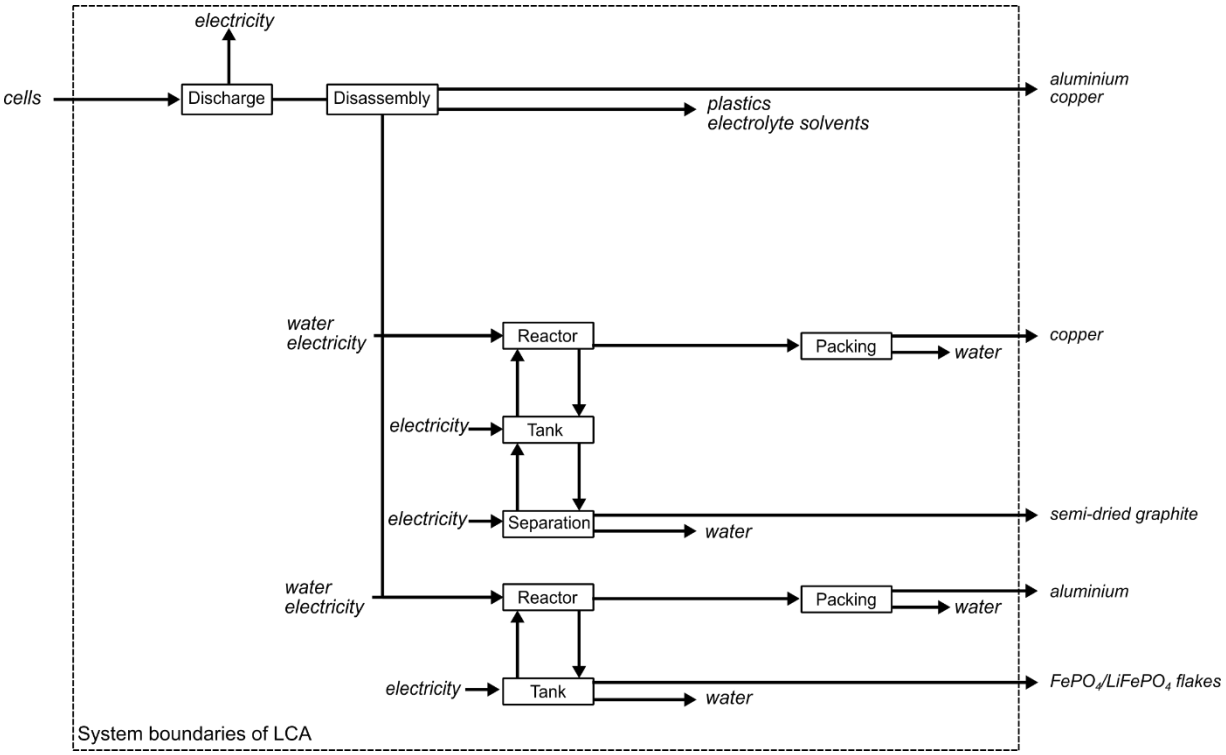

Figure 14: System boundaries (dotted rectangle) of the present LCA study, showing the main steps involved in the KYBURZ recycling process and its most important material and energy flows.

2.3.1. Scenario definition

To reflect seasonal variations in energy demand due to the different ambient temperature, and different water recirculation strategies, four scenarios have been analysed in the frame of the present study. In winter, more electricity is required to heat the process environment to reach the necessary operating temperatures, as ambient conditions are colder. Conversely, during the summer season, higher ambient temperatures reduce the need for heating, resulting in lower electricity consumption. To model these seasonal effects, two main scenarios are defined: *w* for winter and s for summer.

Additionally, within each season, two water recirculation strategies have been considered. In the full recirculation scenarios (*w0* and *s0*), water is assumed to remain in a closed loop, with losses occurring only through the residual moisture on the recovered active layer materials and current collectors. These losses are compensated by reintroducing an equivalent amount of fresh water as input. In contrast, the 5-cycle recirculation scenarios (*w5* and *s5*) assume that water is reused five times before it becomes ineffective for delamination and must be replaced in its entirety. Hence, for this latter scenario, the total input of water is distributed across five reuse cycles before being replaced.

2.3.2. Assumptions and modelling choices

Most of the electrolyte is assumed to be lost during cell operation over a 10-year use period in a KYBURZ vehicle. Particularly because the cells used in the process have a plastic casing that offers low barrier properties to electrolyte solvent permeation. As a result, the cells are often dry upon opening. In contrast, when metallic cell housing is used in the future, its superior barrier properties against electrolyte solvent permeation is expected to preserve more electrolyte. For the portion of electrolyte that remains, it is

assumed that it consists mainly of organic solvents. These solvents either evaporate during processing with the LIBERTY 1.0 machine, where they are captured by the facility's ventilation system, or are removed and treated via incineration. Both of these options are further discussed within the LCA results (compare section 2.3.3). Plastics from both the cell housing and separator, are treated as waste and need to be incinerated.

Regarding the active materials, graphite losses within the system amount to 1 % of the initial input. In scenarios w0 and s0, it is assumed that this 1 % fraction remains entirely attached to the current collector, whereas in scenarios w5 and s5, a split is assumed: 50 % remains attached to the collector, and 50 % is lost through the wastewater stream. For the LFP material, total losses are estimated at 0.5 % of the initial amount, with the same assumption applied across scenarios w0, s0, w5, and s5.

The KYBURZ process results in four secondary material fractions that can be sold to third parties and reintroduced into further use: aluminium, copper, semi-dried graphite and $FePO_4$/$LiFePO_4$ flakes.

- The aluminium and copper fractions are derived from terminals and current collectors. These fractions are collected and sent to external recyclers, with an assumed transport distance of 250 km.
- Graphite is recovered in a semi-dried state from the negative electrodes after delamination in the reactor and sedimentation of active layer flakes in a buffer tank. This is followed by process water separation to further reduce water content, resulting in semi-dried graphite with 70% dryness. This semi-dried graphite is assumed to be sold to external partners, with a transport distance of 250 km
- $FePO_4$/$LiFePO_4$ is recovered as semidried flakes from the positive electrodes after delamination in the reactor and sedimentation in a buffer tank. The output are semi-dried $FePO_4$/$LiFePO_4$ flakes with a dryness of 54%, assumed to be sold to external partners, with a transport distance of 500 km.

2.3.3. Life cycle impact assessment – KYBURZ direct battery recycling process

The LCA study was conducted using the Activity Browser software. For the impact assessment, the Environmental Footprint (version EF 3.0, without long-term effects) method was applied, developed by the European Commission's Joint Research Centre (JRC), comprising 16 different impact categories (ranging from resource use to human toxicity). In addition, the EF single score is calculated. The single score aggregates all 16 impact categories into a single value through normalization and weighting [31]. This approach allows for a more comprehensive comparison of the overall environmental performance of the process, and it allows to get a first idea of the relevance of the various impact categories. Among the 16 impact categories of the EF method, climate change (CC) measured via the global warming potential (GWP) shows the largest contribution, accounting for 66 % of the total single score. In addition, resource use-fossil (RU-f) (9 %), ecotoxicity (ETOX) (6 %), and particulate matter (PM) (4 %) are identified as the next most relevant categories.

Furthermore, the total value of the so-called "Umweltbelastungspunkte" (UBP, according to the Ecological Scarcity 2013, again excluding long-term effects) were calculated in this study. The UBP method is particularly suitable for the Swiss context because of the specific assumptions and characterization factors it incorporates.

The LCA study consists of four scenarios - w0, s0, w5, and s5 - reflecting seasonal variations (winter and summer) and different water recirculation strategies. Results are presented in Table 9. Scenario s0 exhibits the lowest single score value, due to lower energy consumption and full water recirculation. This trend was also confirmed by the UBP results. The minimum relative difference between scenario s0 and the other scenarios is 2 % compared to w0, indicating that seasonal variations have only a minor influence on the overall environmental performance. In contrast, the maximum difference is 18 % for scenario w5 compared to scenario s0, indicating that operational variations (i.e. water recirculation strategy). have a greater influence on the system.

Table 9: EF single score, UBP total and values for the four selected impact categories: climate change (CC), ecotoxicity (ETOX), resource use-fossil (RU-f) and particulate matter (PM) of KYBURZ' direct battery recycling process treating 1 kg of EoL LFP battery cell, for the four scenarios analyzed. Scenarios: s for summer, w for winter, 0 for full water recirculation and 5 for complete water exchange after 5 cycles.

Scenario	EF 3.0, Single score [points]	UBP total [ecopoints]	CC [kg CO_2-eq,]	ETOX [CTUe]	RU-f [MJ, net calorific value]	PM [desease incidence]
w0	2.98E-05	4.78E+02	7.61E-01	3.67E+00	2.07E+00	8.19E-09
w5	3.46E-05	4.95E+02	7.64E-01	1.29E+01	2.10E+00	8.45E-09
s0	2.92E-05	4.72E+02	7.59E-01	3.59E+00	1.89E+00	8.11E-09
s5	3.39E-05	4.89E+02	7.63E-01	1.28E+01	1.92E+00	8.37E-09

2.3.4. Hotspot analysis

Figure 13 shows the results of these 4 EF impact categories as well as of the total UBP, split into the contributions of the various process steps.

The environmental contributions across all 16 EF impact categories, along with the aggregated UBP total results for scenario w0 are presented in Table 16 in the Appendix.

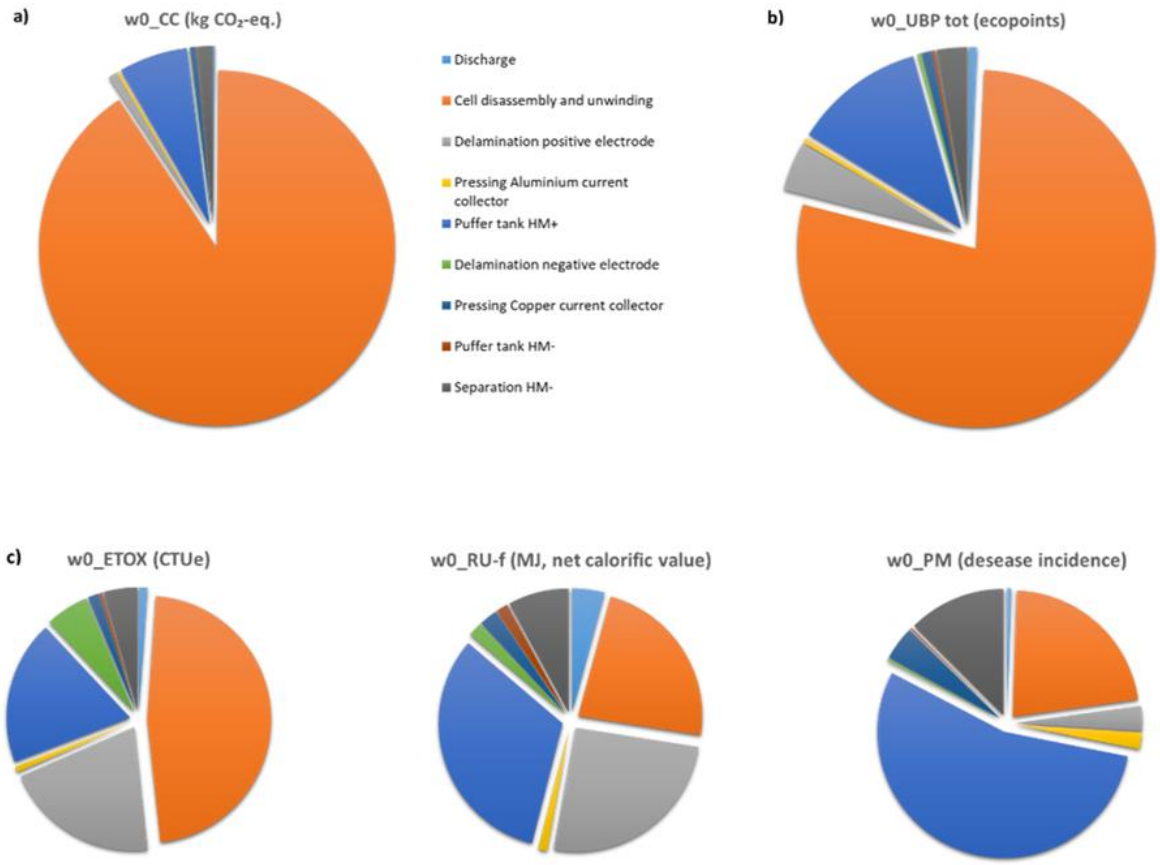

Process steps	w0				
	CC	ETOX	RU-f	PM	UBPtot
Discharge	-0.1 %	-1.1 %	-4.6 %	-0.5 %	-0.74 %
Cell disassembly and unwinding	90.8 %	48.2 %	25.4 %	22.5 %	79.40 %
Delamination positive electrode (reactor)	0.8 %	20.6 %	27.7 %	3.2 %	4.45 %
Pressing Aluminium current collector	0.2 %	0.7 %	1.2 %	2.1 %	0.46 %
Buffer tank HM+	6.3 %	19.3 %	35.2 %	55.1 %	12.04 %
Delamination negative electrode (reactor)	0.1 %	5.8 %	2.1 %	0.3 %	0.34 %
Pressing Copper current collector	0.5 %	1.5 %	2.6 %	4.4 %	0.93 %
Buffer tank HM-	0.0 %	0.4 %	1.7 %	0.2 %	0.28 %
Separation HM-	1.4 %	4.5 %	8.7 %	12.6 %	2.85 %

Figure 15: Shares of the environmental impacts of individual steps of direct recycling technology developed at KYBURZ (scenario w0), treating 1 kg of EoL LFP battery cell, quantified for: a) climate change impact category (EF v3.0), b) UBP total, normalized to the respective maximum value, c) ecotoxicity (ETOX), resource use-fossil (RU-f) and particulate matter (PM) impact categories.

In all scenarios, the discharge step shows a negative contribution to the environmental impact, as the discharged energy is fed back into the grid, replacing the Swiss electricity mix and thereby getting a credit for the related, avoided impacts. The discussion focuses here on scenario w0, which represents current operations with full water recirculation during winter conditions. Regarding the carbon footprint, the total GWP associated with the treatment of 1 kg of LFP battery cell amounts to 0.76 kg CO_2-eq.

The most impactful phase, consistently across all scenarios, is the cell disassembly and unwinding phase, responsible for approximately 91 % (with 0.69 kg CO_2-eq) of the total GWP (see Figure 15 a & b). This is primarily due to the incineration of plastic components from the cell housing and separator (e.g. polyethylene, polypropylene and polyethylene terephthalate), and to a lower extent, incineration of electrolyte entrapped within these plastic fractions. The incineration of plastics alone results in approximately 0.61 kg CO_2-eq. emissions, highlighting a critical hotspot. This finding is consistent across both the EF and UBP assessments. Substituting incineration with plastic recycling could potentially reduce the GWP score. A rough estimate, based on the assumption that recycling of 1 kg of plastics requires 0.7 kWh of electricity [32], suggests that recycling 0.256 kg of plastic would generate only 0.0059 kg CO_2-eq. Therefore, transitioning to metal-based cell housings would minimize plastic usage and associated incineration impacts, as metals can also be recycled. Electrolyte incineration results in the emission of 0.07 kg CO_2-eq. As alternative end-of-life treatment it was assumed that the electrolyte mass flow consists of organic solvents, that would evaporate and be emitted into the atmosphere as volatile organic compounds. Under this assumption, the total GWP of the recycling process increases to 0.81 kg CO_2-eq.

If the impacts related to plastic incineration and/or electrolyte VOC emissions are neglected, thus considering the KYBURZ process without end-of-life treatment of plastics and electrolytes, the GWP is significantly reduced to 0.07 kg CO_2-eq.

Figures 13a and 13b illustrate that the buffer tank for the deposition of the positive harvested mass, is the second-largest contributor. This is mainly due to the transportation burden associated with the recovered LFP flakes.

The electricity consumption associated with the direct recycling operations is low. After accounting for the credit from the energy obtained by discharging of cells, the net electricity consumption is 0.23 kWh/kg cell in winter and 0.18 kWh/kg cell in summer. These translate to emissions of 0.008 kg CO_2-eq (27.5 UBP) and 0.006 kg CO_2-eq (21.5 UBP), respectively. Overall, seasonal variations between summer and winter operation do not significantly affect the environmental impacts. Among all recycling steps, the delamination of positive electrode materials exhibits the highest energy demand. This is because the treatment of cathode materials is non-exothermic and requires continuous external heating to maintain the target temperature (30 °C), whereas anode delamination is an exothermic process, allowing the heating system to be switched off once the reaction starts (compare section 2.1.2). As a result, the impact associated with positive electrode delamination is higher.

Besides the climate change impacts, other impact categories were analysed (see Figure 13c), here the steps that contribute most significantly to the environmental impact are primarily two: the disassembly and unwinding phase and the buffer tank deposition phase, although the distribution of impacts varies depending on the impact category analyzed:

- Ecotoxicity category is mainly driven by the impacts associated with the disassembly and unwinding phase (48 %) for the incineration of plastics, followed by the delamination step (29 %) because of the emissions linked to the production of deionized water, and by the buffer tank deposition step (19 %), due to emissions associated with transportation, especially considering the longer distance assumed for LFP (500 km) compared to graphite (250 km)
- Resource use-fossils category is predominantly affected by the impacts associated with transportation. Consequently, the buffer tank deposition of the positive active material, accounts for

about 28 % of the RU-f impact. Additionally, the delamination of positive electrodes contributes 25 %, driven by the resource use associated with electricity production.

- Particulate matter formation is also mainly linked to transportation emissions, with particulates being released into the air.

The overall impact of the KYBURZ direct battery recycling process is relatively low, particularly when considering several key factors. A significant portion of the total GWP is attributed to plastic incineration, which could be mitigated through material substitution (e.g. metal housing). Additionally, the recycling process itself exhibits very low energy consumption, and since it utilizes the Swiss electricity mix which is characterized by low carbon intensity, this results in a low carbon footprint. Water use in the process contributes minimally to the environmental burden, as water is reused over multiple cycles. Future impacts are expected to slightly rise from adding a cantilever belt for an automatic feeding system of the electrodes and a ventilation system for the delamination process. Their impact is expected to contribute only negligible to the whole energy consumption of the process.

2.3.5. Comparison with other battery recycling processes

A comparative evaluation of existing recycling processes - hydrometallurgical, pyrometallurgical and direct recycling - was conducted to benchmark the results obtained for the KYBURZ direct recycling process.

Several studies have assessed the environmental performance of LIB recycling, covering various chemistries and recycling technologies. However, direct comparison across studies is challenging due to differences in assumptions regarding process configurations, quality of recovered materials, system boundaries, and modelling choices, including background data sources and life cycle impact assessment (LCIA) methods applied.

Reported greenhouse gas (GHG) emissions for recycling 1 kg of battery pack or cells vary widely, from as low as 0.158 kg CO_2-eq. up to 48.8 kg CO_2-eq. [33]. Some studies focus on battery packs, including additional components (e.g., casing, BMS), complicating direct comparison with cell-based assessments. Furthermore, the use of different LCIA methods, such as, IPCC [34], ReCiPe [35], or TRACI [36] or assessment tool such as GREET (Greenhouse gases, Regulated Emissions, and Energy use in Technologies) [37], introduces additional variability.

Table 10 summarizes selected GHG emissions values reported in the literature for hydro-, pyrometallurgical and direct recycling processes, specifically referring to per kilogram of battery cells.

Table 10: Comparison of GHG emissions per kg of LFP cell recycled among different studies.

	Hydrometallurgy [kg CO_2-eq]	**Pyrometallurgy** [kg CO_2-eq]	**Direct** [kg CO_2-eq]
Xu et al. (2020) [20]	2.2	2.4	0.6
Kallitsis et al. (2020) [38]	1.4	1.84	-
Dunn et al. (2022) [39]	2.0	1.8	1.5

Overall, a trend emerges where direct recycling typically shows lower GHG emissions compared to hydro- and pyrometallurgical approaches, although significant variability remains. This underscores the importance of carefully considering system boundaries and methodological assumptions when comparing results.

When comparing the GHG emissions results obtained for the KYBURZ direct recycling process to the values reported in Table 10, it is evident that the KYBURZ process is highly competitive. The GHG emissions are significantly lower than those typically reported for hydro- and pyrometallurgical routes and fall within or below the lower range of values observed for other direct recycling approaches. Especially if we consider that out of the calculated 0.76 kg CO_2-eq./kg LFP cell treated, most of the impact is coming from the incineration of plastic, and that the impact associated to the recycling process has a minor contribution (0.07 kg CO_2-eq./kg LFP cell treated).

To explore the sustainability advantages of KYBURZ' direct battery recycling process in comparison to other recycling processes, an additional assessment was conducted by modelling the life cycle inventories for hydro-, pyrometallurgical and direct recycling routes using the EverBatt 2023 model [40]. The EverBatt model is an excel-based battery recycling process and supply chain model, developed by Argonne National Laboratory [41]. The 2023 version of this model has substantial improvements compared to previous versions, particularly in the modelling of a generic preprocessing step required to generate the black mass required for both, the hydrometallurgical and the direct recycling models. In these two routes, the battery cells undergo a pretreatment stage to isolate the black mass prior to subsequent processing. In contrast, the pyrometallurgical process modeled here does not require a separate preprocessing stage, as the cell is fed directly into the furnace. The corresponding generic process flowcharts for all three pathways are provided in Figure 21 to Figure 24 in Appendix 7.6.

To ensure comparability with the analysis done for the KYBURZ process, the LCIs were built using the same LFP cell composition and mass, with Switzerland as geographical context and using the same functional unit. Accordingly, the Swiss electricity mix (market for electricity, medium voltage, CH) and the same transportation distances as in the previous analysis were used for the output materials.

For all three modeled processes, hydrometallurgical, pyrometallurgical and direct recycling, the recovery of both anode and cathode materials is included. Default material and energy demands per kilogram of recycled cells, as reported in [40], were applied. Furthermore, the energy recovered during the cell discharge step, following the calculation done for the KYBURZ process, was incorporated into all modeled pathways.

In the EverBatt-based direct recycling model, the plastic parts are incinerated, and the resulting CO_2 emissions are directly calculated within the model. This modelling approach differs from the previous analysis, where the impacts of plastic incineration were assessed using corresponding ecoinvent data. Furthermore, aluminum, copper, graphite, and LFP are recovered with a recovery efficiency of 90% assumed for all these materials and across the processes, except for the pyrometallurgical recycling, where a 95 % recovery rate is assumed for copper. Consequently, this leads to different quantities of recovered materials compared to the KYBURZ recycling process, which is characterized by low material losses, as described in paragraph 2.3.2.

Table 11 summarizes the materials recovered for each recycling technology, modeled according to EverBatt model and the KYBURZ direct recycling process.

Table 11: Materials recovered for hydrometallurgical, pyrometallurgical and direct recycling processes modeled according to EverBatt model and the KYBURZ direct battery recycling process treating 1 kg of EoL LFP battery cell.

Recovered materials [kg/kg LFP cell]	Hydrometallurgy	Pyrometallurgy	Direct	direct KYBURZ
aluminum	0.053		0.053	0.059
copper	0.111	0.117	0.111	0.124
graphite	0.167		0.167	0.195
lithium carbonate	0.063			
LFP			0.267	0.331
total output (Al+Cu+graphite+LFP)	*0.331*	*0.117*	*0.60*	*0.71*

The quality and the purity of the output materials are not explicitly specified in the model. Although a relithiation step for LFP is indicated in the flowchart of direct recycling, which is assumed to involve lithium hydroxide as the relithiation agent, no information is provided for other materials. Therefore, no additional post-treatment processes are considered for any route. This assumption is also valid for the KYBURZ process, where recovered semi-dried graphite and LFP flakes are sold without further treatment. In practice, a small fraction of the materials might be lost during relithiation or regeneration; however, because these post-treatment steps fall outside the defined system boundary, no material losses are accounted for in this study.

2.3.6. Life cycle impact assessment – comparison of processes

The EverBatt model was used exclusively to determine the input and output flows required to model the LCI (e.g. material and energy flows) of the three recycling processes: hydrometallurgical, pyrometallurgical, and direct recycling. For the calculation of the environmental impacts associated with the material and energy production, again the ecoinvent database and the EF v3.0 impact assessment method was utilized within the Activity Browser software. Figure 14 shows the same selected EF impact categories and the aggregated environmental impact category (total UBP points) as previously analyzed in section 2.3.4, for each recycling route.

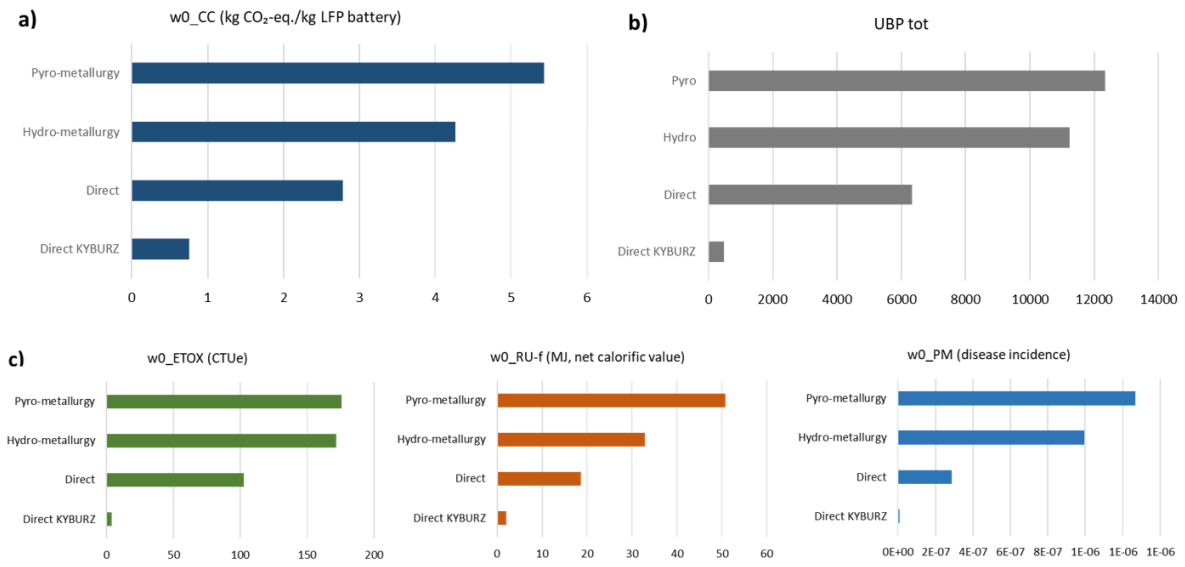

Figure 16: Potential environmental impacts of pyrometallurgical, hydrometallurgical, direct and KYBURZ direct processes, quantified for: a) climate change (CC) impact category, b) UBP total, c) ecotoxicity (ETOX), resource use-fossil (RU-f) and particulate matter (PM) impact categories.

Because the output materials differ between these different recycling technologies (see Table 11), a basket of products approach was adopted for a fair comparison. This approach consists in modelling the same sum of outputs across different systems. For each system, missing output is added as being generated via respective alternative (virgin) production pathways. In this case, the output materials recovered through the KYBURZ direct recycling process (aluminum, copper, graphite and LFP) serve as the reference basket. Materials included in the basket are highlighted in grey in Table 11, and the corresponding environmental impacts are presented in Figure 16.

As a general trend, it can be observed that the KYBURZ direct recycling process shows lower impacts across all categories compared with the other recycling technologies. Specifically, it leads to approximately four times lower GWP than direct recycling, six times lower than hydrometallurgy and seven times lower than pyrometallurgy. The impacts associated to the categories of ecotoxicity, resource use-fossils, and particulate matter of the KYBURZ direct recycling process are reduced by approximately two to three orders of magnitude compared to the other three recycling routes. Since the trend across all impact categories and UBP is nearly identical, the following discussion focuses on the results for GWP.

One of the reasons for the lower impacts of the KYBURZ recycling process lies in the basket of products approach adopted: the reference basket consists directly of the output materials recovered by the KYBURZ process itself, no additional virgin production of materials is needed for its output. In contrast, the other recycling routes (e.g., direct, hydro-, and pyrometallurgical treatments, modelled using EverBatt model), require the additional manufacturing of materials that are not recovered within the respective process (i.e. aluminium, copper, graphite and LFP), contributing substantially to the overall GWP: 24 % for direct recycling, 53 % for hydrometallurgy, and 69 % for pyrometallurgy. In the case of direct recycling, all four materials are recovered (i.e. aluminium, copper, graphite, and LFP), however at 90 % efficiency only. To match the quantities defined in the reference basket (i.e. the output materials from the KYBURZ process), the remaining amount of each material is included through primary production. Similarly, hydrometallurgy recovers aluminium, copper and graphite at 90 % efficiency. In this process, lithium carbonate is recovered rather than LFP. So, the primary production of LFP must be considered, with the recovered lithium carbonate serving as a partial input for this production. To account for this,

the datasets for lithium iron phosphate and its precursors sourced from ecoinvent, were modified accordingly. The pyrometallurgical process recovers copper, meaning that aluminium, graphite, and LFP are fully obtained through primary production to meet the amounts of the reference basket. The total environmental impacts vary considerably depending on the specific materials that each process is able to recover, as well as their respective recycling efficiencies. The KYBURZ process, which achieves high recovery rates and recovers almost all the cell components, shows comparatively lower environmental burdens.

Table 12: Material and energy inputs for recycling 1 kg of EoL LFP battery cell via hydrometallurgical, pyrometallurgical and direct recycling.

	Hydrometallurgy	Pyrometallurgy	Direct recycling
Material [kg]			
nitrogen	5.0E-02		5.0E-02
lime	3.8E-02	0.05	3.8E-02
sulfuric acid	9.2E-02	1.9E-01	
hydrogen peroxide			
hydrochloric acid			
soda ash	1.0E-01		
limestone		1.2E-01	
sand		1.9E-01	
lithium hydroxide			1.4E-02
tap water	7.9E+00	3.8E+00	4.2E+00
flue dust		2.5E-02	6.0E-03
slag		3.4E-01	
waste (solid)	8.1E-01		4.4E-01
Wastewater [m^3]	8.1E-03	5.0E-03	4.2E-03
Energy			
diesel [MJ]	1.2E+00	6.0E-01	1.2E+00
natural gas [MJ]	3.3E+00	1.2E-01	2.8E+00
electricity [kWh]	2.8E-01	3.6E-01	1.3E+00
Transportation [tkm]			
market for transport, lorry, freight	8.3E-02	2.9E-02	2.2E-01

Moreover, a significant portion of the remaining impact in all processes derives from direct emissions associated with the incineration of non-recovered materials, such as plastics, electrolyte, and, in the case of pyrometallurgy, also graphite. This contribution amounts to 57 % of the total impact in direct recycling, 37 % in hydrometallurgy, and 29 % in pyrometallurgy. Another factor leading to the higher

impacts in hydro-, and direct recycling processes is the greater energy demand, including the preprocessing steps necessary to produce black mass, as shown in Table 12. In this regard, it should be noted that, according to the modelling assumptions used in EverBatt 2023, pyrometallurgy does not involve black mass production, therefore it results in a lower reported energy consumption compared to hydro- and direct recycling. This characteristic is inherent to the pyrometallurgical approach modelled here, rather than indicative of a generally higher energy efficiency of the process.

Similarly, the KYBURZ's recycling process enables an effective disassembly of LIB's into high-purity material fractions without requiring the production of black mass, thereby avoiding the energy-intensive preprocessing steps. Europe's current treatment capacity is insufficient to process the quantities of black mass generated [5], and as a result, it is shipped outside of Europe for further processing. This long-distance transport can significantly increase the associated environmental impacts, however, in current model, no transport is assumed for black mass in the hydrometallurgical route.

The use of solvents also contributes to the overall environmental burden of the three processes. For instance, in the modeled direct recycling route, the production of lithium hydroxide accounts for approximately 8 % of the total impact, while in the hydrometallurgical route, the use of sulfuric acid and soda ash contributes approximately 3 %. Differently, for the ecotoxicity impact category, where the use of chemicals results in hydrometallurgy having an impact nearly as high as that of pyrometallurgy.

Overall, the comparison confirms that direct recycling as performed by KYBURZ offers a substantial reduction of the carbon footprint of LFP battery recycling. In particular, the avoidance of chemical use, low energy demand, elimination of energy-intensive pre-treatment for black mass production, and the direct recovery of both graphite and LFP, contribute significantly to the reduced environmental impacts observed. This evaluation does not capture the full footprint of a fully closed-loop recycling system, as the post-treatment of recovered materials, such as LFP relithiation or graphite regeneration are excluded from the system boundaries. Including the post-treatment steps would lead to higher environmental impacts, primarily due to thermal and chemical treatments needed to restore materials to battery-grade quality. Similarly, recovered copper and aluminum would need to be remelted before being reused in the production of a new battery.

Further considerations on marketable output materials

KYBURZ' recycling process generates several secondary materials, including aluminium, copper, graphite, and LFP, which have the potential to re-enter the battery value chain as substitutes for the respective primary raw materials. However, nowadays not all of these recovered materials are actually reintegrated into battery manufacturing. Nevertheless, their recovery also then reduces environmental impacts by reducing the need for energy- and resource-intensive primary production in further application areas for these materials.

For instance, recovered aluminium and copper are sent to respective smelters for conventional recycling of these two materials. This practice enables significant energy savings: recycling aluminium and copper can reduce energy demand by up to 95.5% [42], [43] and 90% [44], [45], respectively, compared to the production of their respective virgin materials.

In the case of graphite, the recovered material is currently being evaluated for its potential use in new anode production as well as potential other applications. Although these applications are still under investigation, they might represent promising opportunities to close material loops within the battery sector.

Similarly, recovered LFP is sent to specialized facilities for testing and potential reprocessing. Preliminary trials on industrial plants have shown that up to 10% of primary LFP can be replaced with recycled material. Ongoing research is focused on improving this share, with the goal of reducing the reliance on virgin material inputs.

2.3.7. Potential climate change benefits by using recycled materials in batteries

This section reports a first estimation of the potential environmental savings achievable by reintroducing all the materials recovered through the KYBURZ recycling process into the battery production cycle as substitutes for primary raw materials. To this end, the system boundaries shown in Figure 14 are expanded beyond the KYBURZ recycling process and include as well the subsequent upgrading steps required in order to enable the reuse of the recovered materials (i.e. aluminium, copper, semi-dried graphite, and LFP flakes) in new batteries. As these additional steps are not executed by KYBURZ (from there, the recovered materials are sold), the modeling is carried out using literature sources and proxies based on assumptions in order to evaluate the impacts of the (additionally) necessary treatment steps.

For this, the global warming potential (GWP) of the upgraded recovered materials (i.e. aluminium, copper, graphite and LFP) is compared with the GWP of the equivalent quantities of primary materials. The (in the KYBURZ recycling process) recovered aluminium from tabs and current collectors is assumed to be remelted by external recyclers and reprocessed into battery-grade products. Here, this has been modelled by using respective ecoinvent datasets for melting and post-processing into battery foil and tabs, using global geography. The resulting GWP for remelting and reprocessing is 0.13 kg CO_2-eq. per 0.059 kg of battery-grade aluminium, whereas producing the same amount of primary aluminium represents an impact of 0.93 kg CO_2-eq.. The copper recovered from tabs and current collectors is refined via electrolytic refining and then converted into battery products, modelled again by using respective ecoinvent datasets. The resulting GWP for refining and reprocessing is 0.41 kg CO_2-eq. per 0.12 kg of battery-grade copper, compared to a value from the primary production of 1.03 kg CO_2-eq.. The semi-dried graphite recovered from the anode fraction requires further processing steps in order to meet battery-grade performance. This includes drying of residual water, modelled following. Piccinno et al. 2016 [46], assuming a global electricity mix, followed by a regeneration step. In the literature, values for regeneration can be found, going from 0.27 to 3.53 kg CO_2-eq. per kg of regenerated graphite in function of the applied process [47]. Hence, the total impact due to drying and regeneration represents a value of 0.10 to 0.70 kg CO_2-eq. per 0.18 kg of regenerated graphite. Producing the same amount of primary graphite leads to 0.76 kg CO_2-eq. (based on average global conditions). Recovered LFP flakes also require reprocessing before reusing in cathode production. This includes drying, again estimated following Piccinno et al. 2016 [46], and a regeneration step. As an industrial regeneration route for recovered LFP is not yet defined and may vary with composition, degradation state, and quality, literature values are used as proxies instead. To approximate the regeneration-related impact, we compare a scenario from the literature which models direct recycling without regeneration [48]; 0.51 kg CO_2-eq. per kg of cathode active material), with two scenarios that include regeneration via hydrothermal relithiation and annealing ([49] 1.18 kg CO_2-eq.; [20] 1.42 kg CO_2-eq. per kg of cathode active material). The difference between these values (i.e. 0.67 to 0.91 kg CO_2-eq.) is indicative and used as a proxy to estimate the impact of the regeneration step. However, this value represents an indicative estimate, as these scenarios may differ in other aspects beyond regeneration alone (e.g., energy mix, process yields, material flows). The resulting GWP is 0.40 to 0.47 kg CO_2-eq per 0.3 kg of regenerated cathode material (with drying and regeneration), while the equivalent primary production emits 1.82 kg CO2-eq (calculated considering average global conditions).

Adding the burdens of these four upgrading steps described above results in 1.03 to 1.70 kg CO_2-eq. of additional emissions. When combined with the actual impacts of the KYBURZ recycling process, this results with a value in the range of 1.79-2.46 kg CO_2-eq. By contrast, producing the respective amounts of primary battery-grade materials (i.e. Al and Cu in the form of foils for the current collectors and LFP and graphite regenerated) results in a value of 4.59 kg CO_2-eq. Hence, based on this comparison, the saving potential is in the order of 2 to 2.5 kg CO_2-eq. per kg of LFP battery.

Within an entire battery cell (with a total climate change impact of 10.63 kg CO_2-eq. per kg when only pristine materials are used for its production), the actual production activities (i.e. electricity and heat consumption, as well as the required infrastructure) represent about 17% of the impact or 1.78 kg CO_2-eq.. The production of all the unrecoverable materials contributes further approximately 40% of the

overall footprint, i.e. an amount of 4.27 kg CO_2-eq.. Figure 17 summarizes all the contributions, distinguishing (i) impacts from processing operations, (ii) impacts from unrecoverable materials, and (iii) impacts associated with the recycling and upgrading operations. Error bars show the impact range (±0.3 kg CO2-eq.) of each contribution across the upgrading steps and the resulting potential savings. Increasing transport efforts in the foreground system (e.g. between the various upgrading places and the cell manufacturing plant) have not been modelled here.

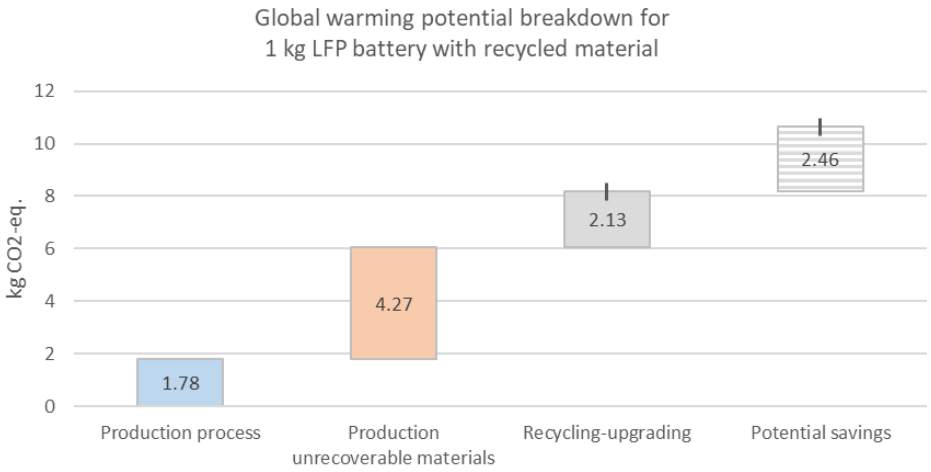

Figure 17: Potential contributions to the climate change impact of producing 1 kg of LFP battery using recycled materi-als, showing impacts from production processes, unrecoverable materials production, recycling/upgrading steps, and potential CO_2-equivalent savings. The figure is based on the assumption of a 100% yield for all the upgrading steps of the recovered materials.

All estimates above are based on an ideal yield for every upgrading step of 100% - i.e. represents in a way the maximum potential. However, this may not reflect the actual industrial practice, where mass losses are common due to inefficiencies in thermal treatments, relithiation and regeneration, or refining. Accordingly, two additional scenarios were evaluated assuming 5 % and 10 % mass losses, respectively, resulting in a saving potential of 2.3 kg CO_2-eq. and 2.1 kg CO_2-eq., respectively. A graphical representation of these two additional scenarios is shown in the Appendix (Figure 25 and Figure 26).

3 Conclusions and outlook

This report summarizes the findings of whole duration of the project which addresses the enhancement of the recycling process for low value LFP LIBs, with a specific focus on high efficiency, sustainability, and economic viability according to the project objectives listed in section 1.2.

First, the SoH of batteries that still allows effective recycling was discussed in section 2.2.2 and appendix 7.3. Since all cells were discharged to the same level it was found that the $FePO_4$/$LiFePO_4$ ratio in the recovered material was around 27:73. This ratio remained independent from the SoH of the processed batteries. Hence, the "quality" of the recovered active material should not be affected by processing batteries of different SoHs. This allows to process cells of various SoHs in one batch and they don't need to be separated according to the SoH prior to processing.

Second, it was found that washing of the electrode materials in a carbonate bath is not necessary for an efficient delamination of the active layer coating from the current collector foils. Additionally, potential emissions of electrolyte components were measured and the reactivity of the electrolyte components in process analysed. The maximum VOC concentration of 31'700 µg/m^3 remained below the advised MAC-value. Other than usually expected, the $LiPF_6$ did not hydrolyse to HF in the water-based process. This can be explained by the chemical behaviour of $LiPF_6$ in aqueous conditions because the PF_6^- anion does not undergo hydrolysis in pure water [12]. Actually, the electrolyte salt was detected as the original PF_6^- anion (31 - 34 mM) with minor formation of POF_nR_{3-n} degradation products (0 - 7 mM).

Third and fourth, a process setup was developed and is described with detailed mass balances for each process step in section 2.1. This final reactor generation allows a total overall recovery rate of 93 %. This recovery was set in context with the recycling efficiencies defined in the EU battery regulation [5]. Since the recovered plastic fractions will be incinerated, they cannot be accounted as "output fractions" for the recycling efficiency according to the battery regulation. Hence, the recycling efficiency ends up at 67.5 % which exceeds the required minimum of 65 % by the end of 2025. The main contribution of the plastic fraction comes from the cell housing. Since there is a clear trend away from plastic cell housings towards metal housings the recycling efficiency will significantly increase once this later metal-case generation will be recycled. Moreover, KYBURZ' recycling process exceeds the demanded targets for the copper and lithium recovery by 10 % respectively 17.7 % already 2.5 years prior to the deadline at the end of 2027 (compare section 2.2.4).

Also, the elemental composition of the process water in the final process setup was analysed and described in section 2.1.4. It was found that even after processing 90 kg of positive electrodes and 148 kg of negative electrodes, the detachment of the active layer coating from the current collector foils still worked unimpaired and thus the water could be reused for further batches. Moreover, the more electrodes that were processed, the higher the lithium concentration accumulates. This effect is more pronounced for the negative electrode process water where a lithium concentration of 1'322 mg/l was achieved after processing 148 kg of electrodes. This concentration is comparable to those found in typical commercial primary lithium brines where concentrations range between 200 and 1'400 mg/l [13]. Ways to recover that lithium will be investigated in a prospective Inno-Cheque project in collaboration with the University of Applied Sciences and Arts Northwestern Switzerland (FHNW). This potential other lithium source could further increase the lithium recovery.

Fifth, a combination of complementary material characterization techniques allowed to determine the composition and quality of the recovered materials as described in section 2.2. Moreover, for the metallic output fractions a potential revenue was estimated. The prices lie between 1.9 and 6.4 $/cell for the worst- and best-case scenario respectively. The active material output fractions were found to be composite materials consisting mostly of active material component. But they also contained ca. 3 – 4 %wt. binder plus conductive additive in the form of graphite or carbon black. The crystallographic condition of both active materials, i.e. $FePO_4$/$LiFePO_4$ and graphite, remained mostly unaffected after material recovery. The microstructure, however, showed some minor and localized artefacts like particle cracking

or impurities. The recovered $FePO_4$/$LiFePO_4$ material achieved only around 70 % of the discharge capacity of primary battery grade $LiFePO_4$. However, it was shown that when adding 10 % wt of the $FePO_4$/$LiFePO_4$ to primary $LiFePO_4$ material of a potential customer, the discharge capacity could be increased by 6-7 % in comparison to their primary $LiFePO_4$ only. This test has been carried out by the potential customer and the result might be explained by using a half-cell setup (i.e. $FePO_4$/$LiFePO_4$ vs. lithium metal), where the $FePO_4$ could be relithiated electrochemically (compare section 2.2.2). For the recovered graphite it is shown above that the material achieves around 85 % of the discharge capacity of primary battery grade graphite (compare section 2.2.3).

Sixth, a Life Cycle Analysis (LCA) including a hot-spot analysis was performed to evaluate the environmental footprint of the process. The LCA assessment confirms that KYBURZ' direct battery recycling process offers a highly promising route to significantly lower the environmental footprint of LFP battery recycling. Key factors contributing to the reduced impacts include the recovery of both graphite and LFP, the avoidance of energy intensive pre-treatment steps, the elimination of chemical-intensive treatments, the low energy demand. Further improvements could be achieved by minimizing plastic incineration, for example by transitioning to metal cell casings or implementing plastic recycling strategies. Relithiation of the $FePO_4$ fraction to $LiFePO_4$ and regeneration of the graphite was not considered within the system boundaries of this LCA, because this treatments will be performed by external third parties that buy KYBURZ' output fractions.

In conclusion, an efficient direct recycling process was developed that allows the recovery of 93 % of the input mass without the formation of black mass. The selective recovery of pure material fractions is a key advantage of KYBURZ' battery recycling process. The guidelines of the EU battery regulation are fulfilled, as the recycling efficiency is over 67.5 % and the rate of recovery for copper and lithium are 100 % and 67 %. The resulting active material output fractions are still intact from a crystallographic point of view. Moreover, the LCA showed that KYBURZ' direct battery recycling process is charged with a lower environmental footprint compared to conventional recycling processes described in literature.

KYBURZ' direct battery recycling process is therefore an interesting alternative to conventional recycling processes like pyro- and hydrometallurgical recycling routes especially for low value materials like LFP cell chemistries. To meet the future demand of recycling capacities for these cell chemistries the process needs further upscaling however. Hence, KYBURZ plans to achieve this by further automatization of the process as well as multiplication (replication) of the production lines.

4 National and international cooperation

Throughout the course of this project, several collaborations and networking opportunities have emerged, driven by the timely and innovative approach to the direct recycling of LIBs. As a result of the project's developments, KYBURZ has taken on a key role in national initiatives such as CircuBAT, as well as in Horizon Europe projects including RESPECT, ReUse and RESTORE projects. Additionally, the collaboration with AWEL on tracing and identification of the trace metals like Cu and Li in process water is highly commendable - prompting KYBURZ and Empa to further collaborate with FHNW on the topic of lithium recovery from process water. In addition, KYBURZ has been collaborating closely with SUVA and continues to do so in assessing and controlling air quality at the recycling facility.

5 Publications and other communications

Table 13: List of publications and other communications including a list of published data and models/codes.

***Title*; published data and models/codes**	**What**	**When**	**Event/Organization**
Regeneration of Cathode Active Material from End-of-Life $LiFePO_4$ Batteries; - Influence of time and temperature of thermal treatments of harvested $LiFePO_4$ material.	Poster	29.09.2022	Swiss Battery Days 2022
Direct Recycling of End-of-Life $LiFePO_4$ Cathodes; - Validation that XRD can be used to reliably determine the $FePO_4$:$LiFePO_4$ ratio - Crystallographic assessment of the harvested $FePO_4$/$LiFePO_4$ material and its relithiated descendents - Electrochemical performance of the $LiFePO_4$ materials	Poster	18.09.2023	Swiss Battery Days 2023
Batterierecycling: Den Kreislauf schliessen	Artikel	24.10.2024	Das Portal der Schweizer Regierung
Characterization and Relithiation of EoL $LiFePO_4$; - Binder identification via thermogravimetric analysis - Quality assessment of harvested $FePO_4$/$LiFePO_4$ material and its relithiated descendents - Aqueous relithiation of harvested $FePO_4$/$LiFePO_4$ material - Electrochemical assessment of $LiFePO_4$ materials	Presentation	11.09.2024	International Congress for Battery Recycling 2024
Direct Recycling of End-of-Life $LiFePO_4$ Cathodes; - Binder identification via thermogravimetric analysis - Quality assessment of harvested $FePO_4$/$LiFePO_4$ material and its relithiated descendents - Aqueous relithiation of harvested $FePO_4$/$LiFePO_4$ material - Electrochemical assessment of $LiFePO_4$ materials	Poster	29.10.2024	Direct Recycling Battery Conference 2024

(Environmental) Sustainability Assessment of Direct Battery Recycling - LCA analysis of KYBURZ direct recycling process - Comparison of KYBURZ direct recycling process vs existing recycling processes	Poster	29.10.2024	Direct Recycling Battery Conference 2024

6 References

[1] International Energy Agency, *Global EV Outlook 2024: moving towards increased affordability*. in Global EV Outlook, no. 2024. OECD, 2024. [Online]. Verfügbar unter: https://www.iea.org/reports/global-ev-outlook-2024

[2] C. Pillot, „The Rechargeable Battery Market and Main Trends 2023-2030“, gehalten auf der ICBR - international congress for battery recycling, Basel, 12. September 2024.

[3] „Nachrichten Batterierecycling“, Battery-News. Zugegriffen: 16. Januar 2025. [Online]. Verfügbar unter: https://battery-news.de/batterie-recycling/

[4] „Business Case Study - LIB value chain“, online.

[5] „Regulation (EU) 2023/ of the European Parliament and of the Council of 12 July 2023 concerning batteries and waste batteries, amending Directive 2008/98/EC and Regulation (EU) 2019/1020 and repealing Directive 2006/66/EC“.

[6] D. Waldmann, „Unlocking the potential: BASF’s vision for successful battery recycling in Europe“, gehalten auf der International Congress for Battery recycling - ICBR 2024, Basel, 12. September 2024.

[7] BATT4EU, „Strategic Research & Innovation Agenda“, Feb. 2024. [Online]. Verfügbar unter: https://bepassociation.eu/our-work/sria/

[8] „COMMISSION DELEGATED REGULATION (EU) …/... supplementing Regulation (EU) 2023/1542 of the European Parliament and of the Council by establishing the methodology for calculation and verification of rates for recycling efficiency and recovery of materials from waste batteries, and the format for the documentation“, [Online]. Verfügbar unter: https://eur-lex.europa.eu/legal-content/EN/TXT/?uri=intcom:C%282025%291674

[9] Y. Zhao *u. a.*, „Precise separation of spent lithium-ion cells in water without discharging for recycling“, *Energy Storage Mater.*, Bd. 45, S. 1092–1099, März 2022, doi: 10.1016/j.ensm.2021.11.005.

[10] „SR 814.201 - Gewässerschutzverordnung vom 28. Oktober 199...“, Fedlex. Zugegriffen: 25. April 2025. [Online]. Verfügbar unter: https://www.fedlex.admin.ch/eli/cc/1998/2863_2863_2863/de

[11] L. Guo, D. B. Thornton, M. A. Koronfel, I. E. L. Stephens, und M. P. Ryan, „Degradation in lithium ion battery current collectors“, *J. Phys. Energy*, Bd. 3, Nr. 3, S. 032015, Juli 2021, doi: 10.1088/2515-7655/ac0c04.

[12] L. Sheng *u. a.*, „Unraveling the Hydrolysis Mechanism of $LiPF_6$ in Electrolyte of Lithium Ion Batteries“, *Nano Lett.*, Bd. 24, Nr. 2, S. 533–540, Jan. 2024, doi: 10.1021/acs.nanolett.3c01682.

[13] V. Balaram, M. Santosh, M. Satyanarayanan, N. Srinivas, und H. Gupta, „Lithium: A review of applications, occurrence, exploration, extraction, recycling, analysis, and environmental impact“, *Geosci. Front.*, Bd. 15, Nr. 5, S. 101868, Sep. 2024, doi: 10.1016/j.gsf.2024.101868.

[14] „Grenzwerte am Arbeitsplatz: Aktuelle MAK- und BAT-Werte“. Zugegriffen: 25. April 2025. [Online]. Verfügbar unter: https://www.suva.ch/de-ch/services/grenzwerte

[15] A. K. Vinayak, Z. Xu, G. Li, und X. Wang, „Current Trends in Sourcing, Recycling, and Regeneration of Spent Lithium-Ion Batteries—A Review“, *Renewables*, Bd. 1, Nr. 3, S. 294–315, Juni 2023, doi: 10.31635/renewables.023.202200008.

[16] „Battery-related waste codes update set to boost circular economy - European Commission“. Zugegriffen: 8. August 2025. [Online]. Verfügbar unter: https://environment.ec.europa.eu/news/battery-related-waste-codes-update-set-boost-circular-economy-2025-03-05_en

[17] „New Regulation on waste shipments enters into force - European Commission“. Zugegriffen: 8. August 2025. [Online]. Verfügbar unter: https://environment.ec.europa.eu/news/new-regulation-waste-shipments-enters-force-2024-05-20_en

[18] „Delegated decision - 2025/934 - EN - EUR-Lex“. Zugegriffen: 8. August 2025. [Online]. Verfügbar unter: https://eur-lex.europa.eu/eli/dec_del/2025/934/oj/eng

[19] C. Karow, „Li-Cycle Files for Insolvency in Canada“, Battery-News. Zugegriffen: 8. August 2025. [Online]. Verfügbar unter: https://battery-news.de/en/2025/05/16/li-cycle-files-for-insolvency-in-canada/

[20] P. Xu *u. a.*, „Efficient Direct Recycling of Lithium-Ion Battery Cathodes by Targeted Healing“, *Joule*, Bd. 4, Nr. 12, S. 2609–2626, Dez. 2020, doi: 10.1016/j.joule.2020.10.008.

[21] V. Palomares *u. a.*, „Conductive additive content balance in Li-ion battery cathodes: Commercial carbon blacks vs. in situ carbon from LiFePO4/C composites“, *J. Power Sources*, Bd. 195, Nr. 22, S. 7661–7668, Nov. 2010, doi: 10.1016/j.jpowsour.2010.05.048.
[22] Z. Yang und S. Wang, „High Cycling Performance Cathode Material: Interconnected $LiFePO_4$ /Carbon Nanoparticles Fabricated by Sol-Gel Method“, *J. Nanomater.*, Bd. 2014, Nr. 1, S. 801562, Jan. 2014, doi: 10.1155/2014/801562.
[23] T. Insinna, E. N. Bassey, K. Märker, A. Collauto, A.-L. Barra, und C. P. Grey, „Graphite Anodes for Li-Ion Batteries: An Electron Paramagnetic Resonance Investigation“, *Chem. Mater.*, Bd. 35, Nr. 14, S. 5497–5511, Juli 2023, doi: 10.1021/acs.chemmater.3c00860.
[24] „REGULATION (EU) 2019/ 1021 OF THE EUROPEAN PARLIAMENT AND OF THE COUNCIL - of 20 June 2019 - on persistent organic pollutants“.
[25] „ISO 14040:2006(en), Environmental management — Life cycle assessment — Principles and framework“. Zugegriffen: 30. April 2025. [Online]. Verfügbar unter: https://www.iso.org/obp/ui/#iso:std:iso:14040:ed-2:v1:en
[26] „ISO 14044:2006(en), Environmental management — Life cycle assessment — Requirements and guidelines“. Zugegriffen: 30. April 2025. [Online]. Verfügbar unter: https://www.iso.org/obp/ui/#iso:std:iso:14044:ed-1:v1:en
[27] „ecoinvent - Data with purpose.“, ecoinvent. Zugegriffen: 30. April 2025. [Online]. Verfügbar unter: https://ecoinvent.org/
[28] B. Steubing, D. De Koning, A. Haas, und C. L. Mutel, „The Activity Browser — An open source LCA software building on top of the brightway framework“, *Softw. Impacts*, Bd. 3, S. 100012, Feb. 2020, doi: 10.1016/j.simpa.2019.100012.
[29] L. Zampori, R. Pant, und European Commission, Hrsg., *Suggestions for updating the organisation environmental footprint (OEF) method*. Luxembourg: Publications Office, 2019. doi: 10.2760/424613.
[30] F. O. for the E. FOEN, „Swiss Eco-Factors 2021 according to the Ecological Scarcity Method“. Zugegriffen: 30. April 2025. [Online]. Verfügbar unter: https://www.bafu.admin.ch/bafu/en/home/themen/thema-wirtschaft-und-konsum/wirtschaft-und-konsum--publikationen/publikationen-wirtschaft-und-konsum/oekofaktoren-schweiz.html
[31] S. Sala, A. K. Cerutti, und R. Pant, „Development of a weighting approach for the Environmental Footprint“.
[32] J. Quan, S. Zhao, D. Song, T. Wang, W. He, und G. Li, „Comparative life cycle assessment of LFP and NCM batteries including the secondary use and different recycling technologies“, *Sci. Total Environ.*, Bd. 819, S. 153105, Mai 2022, doi: 10.1016/j.scitotenv.2022.153105.
[33] J. Li, L. Li, R. Yang, und J. Jiao, „Assessment of the lifecycle carbon emission and energy consumption of lithium-ion power batteries recycling: A systematic review and meta-analysis“, *J. Energy Storage*, Bd. 65, S. 107306, Aug. 2023, doi: 10.1016/j.est.2023.107306.
[34] Intergovernmental Panel on Climate Change (IPCC), *Climate Change 2021 – The Physical Science Basis: Working Group I Contribution to the Sixth Assessment Report of the Intergovernmental Panel on Climate Change*. Cambridge: Cambridge University Press, 2023. doi: 10.1017/9781009157896.
[35] M. A. J. Huijbregts *u. a.*, „ReCiPe2016: a harmonised life cycle impact assessment method at midpoint and endpoint level“, *Int. J. Life Cycle Assess.*, Bd. 22, Nr. 2, S. 138–147, Feb. 2017, doi: 10.1007/s11367-016-1246-y.
[36] O. US EPA, „Tool for Reduction and Assessment of Chemicals and Other Environmental Impacts (TRACI)“. Zugegriffen: 30. April 2025. [Online]. Verfügbar unter: https://www.epa.gov/chemical-research/tool-reduction-and-assessment-chemicals-and-other-environmental-impacts-traci
[37] „GREET“, Energy.gov. Zugegriffen: 30. April 2025. [Online]. Verfügbar unter: https://www.energy.gov/eere/greet
[38] E. Kallitsis, A. Korre, und G. H. Kelsall, „Life cycle assessment of recycling options for automotive Li-ion battery packs“, *J. Clean. Prod.*, Bd. 371, S. 133636, Okt. 2022, doi: 10.1016/j.jclepro.2022.133636.
[39] J. Dunn, A. Kendall, und M. Slattery, „Electric vehicle lithium-ion battery recycled content standards for the US – targets, costs, and environmental impacts“, *Resour. Conserv. Recycl.*, Bd. 185, S. 106488, Okt. 2022, doi: 10.1016/j.resconrec.2022.106488.
[40] „EverBatt“, Argonne National Laboratory. Zugegriffen: 30. April 2025. [Online]. Verfügbar unter: https://www.anl.gov/amd/everbatt

[41] Q. Dai, J. Spangenberger, S. Ahmed, L. Gaines, J. Kelly, und M. Wang, „EverBatt: A Closed-loop Battery Recycling Cost and Environmental Impacts Model“, ANL--19/16, 1530874, 153050, Apr. 2019. doi: 10.2172/1530874.
[42] „Aluminium recycling saves 95% of the energy needed for primary aluminium production“, International Aluminium Institute. Zugegriffen: 24. Juni 2025. [Online]. Verfügbar unter: https://international-aluminium.org/landing/aluminium-recycling-saves-95-of-the-energy-needed-for-primary-aluminium-production/
[43] W. Wei, „Energy Consumption and Carbon Footprint of Secondary Aluminum Cast House“.
[44] „Recycling - International Copper Association“, https://internationalcopper.org/. Zugegriffen: 24. Juni 2025. [Online]. Verfügbar unter: https://internationalcopper.org/policy-focus/climate-environment/recycling/
[45] „Copper Environmental Profile - International Copper Association“, https://internationalcopper.org/. Zugegriffen: 24. Juni 2025. [Online]. Verfügbar unter: https://internationalcopper.org/sustainable-copper/about-copper/copper-environmental-profile/
[46] F. Piccinno, R. Hischier, S. Seeger, und C. Som, „From laboratory to industrial scale: a scale-up framework for chemical processes in life cycle assessment studies“, *J. Clean. Prod.*, Bd. 135, S. 1085–1097, Nov. 2016, doi: 10.1016/j.jclepro.2016.06.164.
[47] S. Natarajan, T. Mae, H. Y. Teah, H. Sakurai, und S. Noda, „Environmentally friendly regeneration of graphite from spent lithium-ion batteries for sustainable anode material reuse“, *J. Mater. Chem. A*, Bd. 13, Nr. 7, S. 4984–4993, 2025, doi: 10.1039/D4TA07618D.
[48] L. Kurz, S. Forster, R. Wörner, und F. Reichert, „Environmental Impacts of Specific Recyclates in European Battery Regulatory-Compliant Lithium-Ion Cell Manufacturing“, *Sustainability*, Bd. 15, Nr. 1, S. 103, Dez. 2022, doi: 10.3390/su15010103.
[49] H. Gao *u. a.*, „Efficient Direct Recycling of Degraded $LiMn_2O_4$ Cathodes by One-Step Hydrothermal Relithiation“, *ACS Appl. Mater. Interfaces*, Bd. 12, Nr. 46, S. 51546–51554, Nov. 2020, doi: 10.1021/acsami.0c15704.

7 Appendix

7.1 Disassembly of battery cells to access the electrodes

The already established KYBURZ cell cutting facility (LIBERTY 1.0) first removes the case lid of the cells. Then, the cells are drilled at the back of the case, and the electrode packs are ejected using compressed air. The cell pack is steered across the roller to separate the main components of the pack i.e., the electrodes (the anode and the cathode) and the separator. This leads to the separate collection of anode and cathode components in two different compartments. The schematic diagram of these process steps is shown in Figure 18.

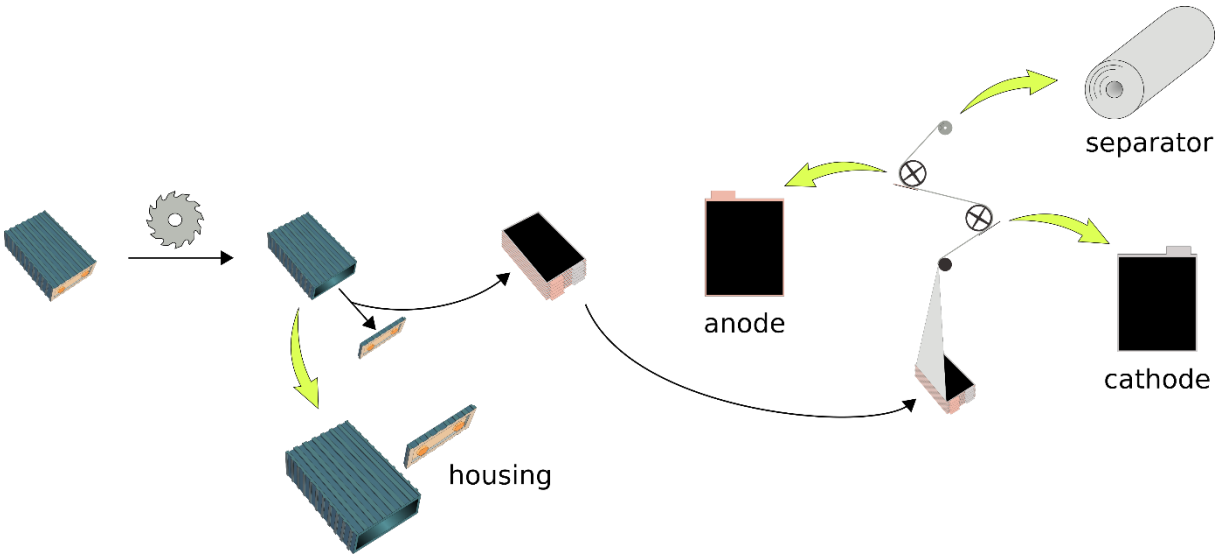

Figure 18: Sketch of cell disassembly and electrode separation using KYBURZ LIBERTY 1.0 system developed in a precedent phase.

7.2 Air quality measurements of previous experiments

In previous steps of the process development, experimental studies were carried out to assess and detect airborne particles originating from the recycling process. Two key steps of the recycling process were examined, this includes the electrode pack separation (unwinding) in the LIBERTY machine and the electrode delamination process in the laboratory. The employed method, a sampling badge with integrated membranes, allows detecting particle masses down to sub-nanogram quantities. The analysis focused on target materials such as LFP powder, graphite powder, and plastic chips from the cell housing. The measurements were conducted in collaboration with an external partner. The sampling was done in three different locations and on four different days which corresponds to one membrane per day.

All membranes were analyzed using a Raman spectroscopy which allowed to quantify material of interest. The Raman signal was collected from a predetermined number of points across the entire membrane area. Results showed the detection of only traces of graphite coexisting with another more dominant carbonaceous species. Neither LFP nor plastic chips from the cell casing were detected in any membrane. During the qualitative inspection of the membranes, the Raman spectra indicate on the one hand the presence of graphite on three membranes (data not shown). However, the corresponding masses of these graphite were in traces and below their limit of quantification (LoQ) which is 5 ng for pure graphite.

On the other hand, another carbonaceous material was identified in significant mass. Due to the dominance of carbon black (CB) like spectra on the respective membrane, commercially available CB (Mitsubishi Chemical Corporation MA100) was used as reference material for the quantitative analysis. The corresponding exposures were calculated based on the detected mass of CB and the total air volume sampled by the badge and resulted at maximum 6.93 x 10^{-2} µg/m^3 if detectable (see Table 14). All the exposures were below the current permissible limit (PEL) of the Occupational Safety and Health Administration (OSHA) in the US for CB, which is 3.5 mg/m^3 as 8-hour time-weighted average (TWA) concentration. In conclusion, the findings indicate minimal graphite presence and carbonaceous material resembling CB below the PEL.

Table 14: Summary of the sampling conditions and details associated to the inspected filtration membranes: Location, effective sampling time [h] at nominal flow rate of 90 ml/min, and exposure results of the inspected filtration membranes. Limit of quantification (LoQ) for the analyzed carbon black (CB) was 1 x 10^{-3} µg.

Location	Day	Sampling time [h]	Respirable exposure to CB [8 µg/m^3]
Laboratory	1	6.08	< LoQ
	2	9.18	< LoD
	3	8.12	< LoQ
	4	8.08	< LoQ
LIBERTY (inside)	1	8.06	6.93 x 10^{-2}
	2	8.85	< LoD
	3	8.20	< LoQ
	4	5.66	5.86 x 10^{-2}
LIBERTY (outside)	1	7.42	< LoQ
	2	9.15	< LoD
	3	7.85	< LoQ
	4	8.00	< LoD

7.3 Phase quantification of harvested $FePO_4$/$LiFePO_4$ material with different histories

During the first phase of this project X-ray powder diffraction (XRD) has been proven to be a reliable method for the crystallographic quality assessment of LiFePO4 within the collected material (i.e. active layer composite consisting of $FePO_4$/$LiFePO_4$, conductive additives (graphite), binder and potential degradation products thereof). On the one hand, XRD allows to identify the state-of-charge of the recovered $LiFePO_4$ which means the fraction of delithiated $FePO_4$ and $LiFePO_4$ can be quantified. On the other hand, XRD allows to assess whether side phases are present in the active material within the collected material. It was found that no side phases were present in the collected material. Moreover, through a full relithiation of the $FePO_4$ active material particles, phase-pure $LiFePO_4$ particles could be restored.

Table 15: Overview and background information of the cells investigated. S1c – S4c represent a batch of cells of various SoH. The prefix "0V" indicates the second batch of cells that either did not show a voltage when collected or were deep discharged to 0 V. For each cell, 30 electrode sheets out of 105 were investigated as a randomly selected subset for a representative sampling.

Cell name	State of health [%]	$U_{intitial}$ [V]	$U_{discharge}$ [V]
S1c	82	3.2	2
S2c	72	3.2	2
S3c	52	3.2	2
S4c	7	3.2	2
0V S5c	-	0	0
0V S1	-	0	0
0V S2	-	0	0
0V S3	-	1.9	0
0V S4	50	3.3	0

The collected material originating from different cells with various SoH were systematically analyzed to evaluate the influence of the SoH on the quality of these output materials. Through this assessment it was possible to evaluate which SoH still allows an effective recycling of the cells. This means, in turn, that if through XRD different material qualities depending on the SoH were identified, the cells should be processed in different batches for the according material quality. If there are no different material qualities on the other hand, all cells can be processed in one and the same waste stream. Besides cells of different SoH, KYBURZ also has many cells for which no voltage can be measured, i.e. so called "0 V cells". Consequently, the SoH of the active material cannot be assessed for these 0 V cells. However, these 0 V cells are also part of the daily EoL cell waste stream which is why additionally several 0 V cells were investigated for their $LiFePO_4$ material quality. As electrodes of one cell do not age uniformly, SoH variations exist between the electrode sheets of a cell or even within areas of the same electrode sheet. To address these differences, electrode sheets of one cell were mixed and 30 electrode sheets out of 105 were investigated as a randomly selected subset for a representative sampling. Table 15 provides an overview of all the cells investigated and their corresponding discharge protocol before disassembly.

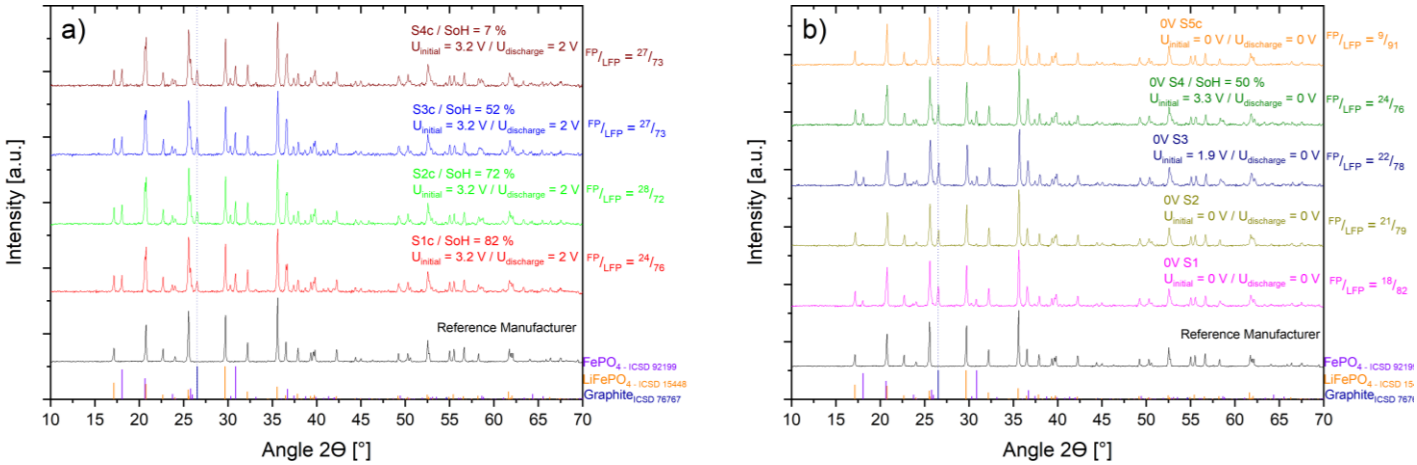

Figure 19: XRD diffraction patterns of collected materials originating from cells of a) different SoH and b) 0 V with different backgrounds. For each cell, 30 electrode sheets out of 105 were investigated as a randomly selected subset for a representative sampling. FP is an abbreviation for $FePO_4$ and LFP for $LiFePO_4$

In Figure 19 a) the diffraction pattern of the collected materials originating from cells of different SoH are depicted. Apart from the graphite (27°) no side phases could be observed. This graphite is used as an electron conductive additive that is added during manufacturing of the cell. For the samples S1-4c (see Table 15) the fractions of the two phases were approximately constant at around 27 % $FePO_4$ and 73 % $LiFePO_4$. Therefore, these samples have no different "grades" of quality for different SoH. Hence, a complete relithiation of the $FePO_4$ fraction in the collected material and therefore effective recycling of the material is feasible.

For the 0 V cells no side phases could be observed, either, and the graphite acting as a conductive agent was also present (see Figure 19 b). Again, the $FePO_4$ and $LiFePO_4$ fractions were relatively constant at around 21 % $FePO_4$ and 79 % $LiFePO_4$. During discharging of a cell, the lithium ions shuttle from the graphite at the negative electrode through the electrolyte to the positive electrode and intercalate into the $FePO_4$ structure on the positive electrode. Hence, it could be expected that the lower the voltage, the more lithium theoretically intercalates into the delithiated $FePO_4$. This might explain the slightly higher level of $LiFePO_4$ fractions in comparison to the samples of Figure 19 a). In conclusion, also for the 0 V cells no differences in the material quality of the collected materials could be identified and the material quality assessed by the XRD pattern of the $LiFePO_4$ is similar between the two batches.

For the material of cell 0 V S5c an $LiFePO_4$ content of 91 % was measured (see Figure 19 b). However, if the material comes from a relatively new cell, that has an internal short circuit due to unknown reasons, the material could still be in a relatively "good" condition and with little loss of lithium inventory and hence high $LiFePO_4$ content. Yet, such a cell would be considered as a real EoL cell that could appear in daily business. Additionally, there is also no side phase observable and a high $LiFePO_4$ content is even more favorable for the relithiation because less lithium source is needed to refill the structure. Moreover, in the final facility, the output material is expected to be a mixture of active layer materials originating from many different cells so that this high $LiFePO_4$ content will be leveled out.

As a conclusion, it was found that independent of the SoH the $FePO_4$/$LiFePO_4$ ratios stayed almost constant. Consequently, the required amount of lithium for the relithiaiton stays almost constant as well. Therefore, from a crystallographic perspective, effective regeneration of the collected material seems feasible. In the context of direct recycling, this approach is advantageous because it eliminates the need for further decomposition, thereby preserving the intrinsic structural integrity of the material. Moreover, it was found that the $FePO_4$/$LiFePO_4$ ratio in the batch from cells of different SoH are similar to the one in the batch of the 0 V cells. This implies that all the EoL cells can be treated within the same waste

stream and that would lead to an estimated $FePO_4$/$LiFePO_4$ ratio around 24/76, varying slightly with the composition of the waste stream i.e., a higher share of 0 V cell increases the $LiFePO_4$ fraction whereas a higher share of cells with a low SoH decreases the $LiFePO_4$ fraction.

7.4 Discharge capacities of recovered $FePO_4/LiFePO_4$ material

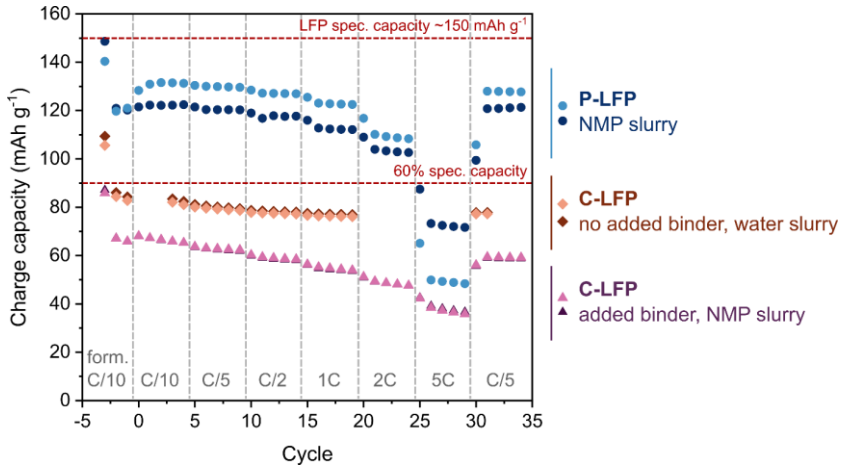

Figure 20: Charge capacity of LFP/graphite cells at different C-rates. The cells differ by their cathodes, which were produced with pristine LFP (P-LFP) in a NMC slurry, recovered LFP (C-LFP) in a NMP slurry and recovered LFP (C-LFP) in a water slurry. The first three cycles correspond to the formation cycles at a C/10 rate. The C-rate for the rate tests are based on the last discharge capacity of each cell measured at the end of formation.

7.5 Potential environmental impact values for 16 impact categories

See Table 16 on page 68.

Table 16: Potential environmental impact values of scenarios w0 representing the KYBURZ direct recycling of 1 kg of LFP in winter with full recirculation of water, for the 16 impact categories of the Environmental Footprint (EF) and the Ecological Scarcity (UBPtot) method. Abbreviations for EF: AC= acidification, CC= climate change, ETOX= ecotoxicity freshwater, RU-f= resource use-fossil, EUT-f= eutrophication freshwater, EUT-m= eutrophication marine, EUT-t= eutrophication terrestrial, HTOX-c= human toxicity cancer effects, HTOX-nc= human toxicity non-cancer effects, IR= ionising radiation, LU= land use, RU-mm= resource use-mineral and metals, OD= ozone depletion, PM= particulate matter, OF= photochemical ozone formation, WU= water use.

	AC	**CC**	**ETOX**	**RU-f**	**EU-f**	**EU-m**	**EU-t**	**HTOX-c**	**HTOX-nc**	**IR**	**LU**	**RU-mm**	**OD**	**PM**	**POF**	**WU**	**UBPtot**
	mol H+-Eq	kg CO2-Eq	CTUe	MJ, net calorific value	kg PO4-Eq	kg N-Eq	mol N-Eq	CTUh	CTUh	kBq U235-Eq	dimen-sionless	kg Sb-Eq	kg CFC-11-EQ	disease inci-dence	NMVOC-Eq	m3 world eq. de-prived	UBP
Discharge	-4.9E-06	-9.6E-04	-4.1E-02	-9.6E-02	-3.8E-08	-8.3E-07	-1.2E-05	-1.3E-12	-2.7E-11	-2.4E-03	-7.3E-03	-1.7E-08	-3.1E-11	-4.2E-11	-3.0E-06	-1.3E-02	-3.5E+00
Cell disassembly and unwinding	2.1E-04	6.9E-01	1.8E+00	5.3E-01	1.7E-06	7.8E-05	8.2E-04	6.8E-11	1.5E-09	2.8E-03	1.1E-01	2.2E-07	5.4E-09	1.8E-09	2.4E-04	3.6E-02	3.8E+02
Delamination cathode	3.1E-05	5.9E-03	7.6E-01	5.7E-01	2.3E-07	5.1E-06	7.2E-05	8.0E-12	1.6E-10	1.4E-02	4.4E-02	1.0E-07	2.6E-10	2.6E-10	1.8E-05	7.9E-02	2.1E+01
Pressing Al cur-rent collector	8.4E-06	1.8E-03	2.7E-02	2.6E-02	1.5E-08	3.3E-06	3.5E-05	1.0E-12	2.6E-11	2.7E-05	1.9E-02	5.8E-09	3.9E-11	1.8E-10	1.2E-05	1.9E-03	2.2E+00
Buffer suspen-sion HM+	2.2E-04	4.8E-02	7.1E-01	7.3E-01	4.1E-07	8.5E-05	9.2E-04	2.7E-11	6.8E-10	2.4E-03	5.0E-01	1.6E-07	1.0E-09	4.5E-09	3.2E-04	1.5E-02	5.8E+01
Delamination anode	2.7E-06	4.7E-04	2.1E-01	4.3E-02	1.9E-08	4.1E-07	5.6E-06	6.4E-13	1.4E-11	1.1E-03	3.4E-03	8.5E-09	4.1E-11	2.3E-11	1.5E-06	5.9E-03	1.6E+00
Pressing Cu current collector	1.7E-05	3.8E-03	5.5E-02	5.3E-02	3.1E-08	6.8E-06	7.3E-05	2.1E-12	5.3E-11	5.6E-05	4.0E-02	1.2E-08	8.1E-11	3.6E-10	2.5E-05	2.1E-03	4.5E+00
buffer suspen-sion HM-	1.8E-06	3.6E-04	1.5E-02	3.6E-02	1.4E-08	3.1E-07	4.4E-06	4.9E-13	9.9E-12	9.0E-04	2.7E-03	6.3E-09	1.2E-11	1.6E-11	1.1E-06	5.0E-03	1.3E+00
separation HM-	5.0E-05	1.1E-02	1.7E-01	1.8E-01	9.8E-08	1.9E-05	2.1E-04	6.2E-12	1.6E-10	8.9E-04	1.1E-01	3.9E-08	2.4E-10	1.0E-09	7.3E-05	5.3E-03	1.4E+01

7.6 Process flow charts from the EverBatt2023 model

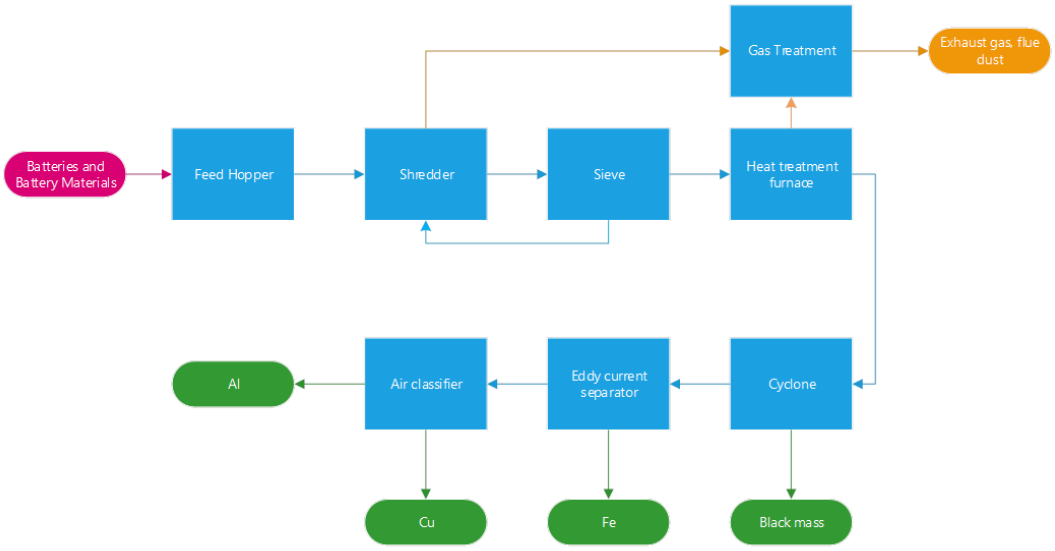

Figure 21: Process flow for the modelled generic pre-treatment process according to EverBatt2023 [40].

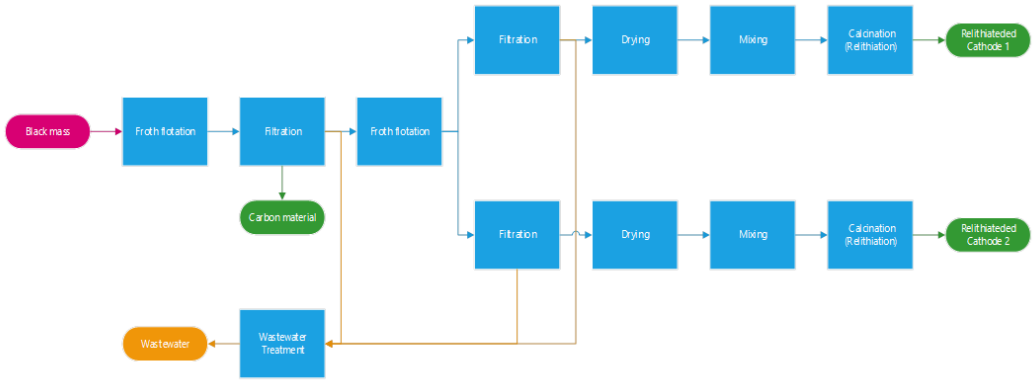

Figure 22: Process flow for the modelled generic direct-based recycling process according to EverBatt2023 [40].

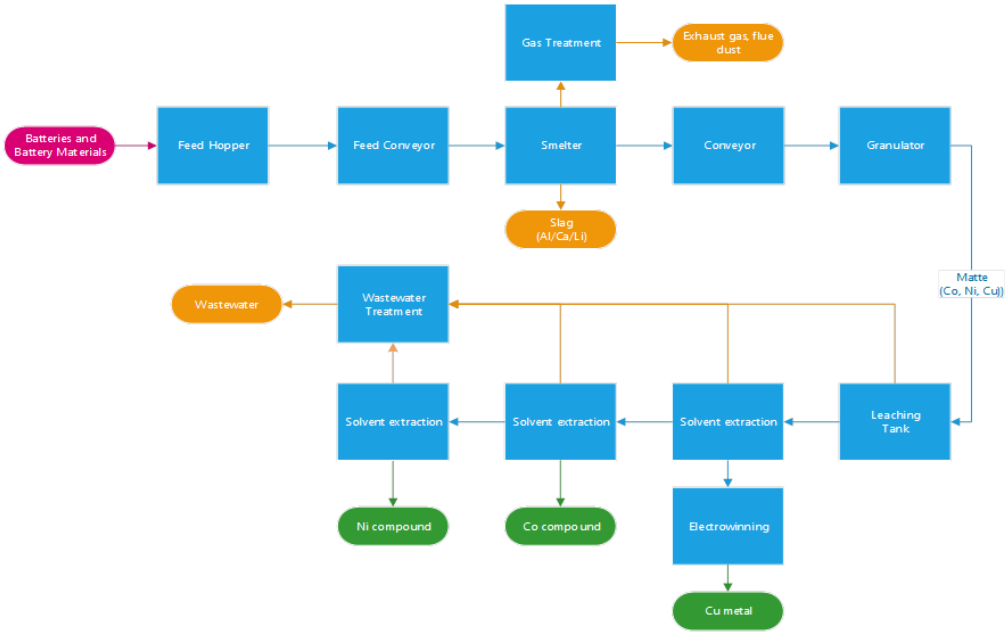

Figure 23: Process flow for the modelled generic hydrometallurgy-based recycling process according to EverBatt2023 [40].

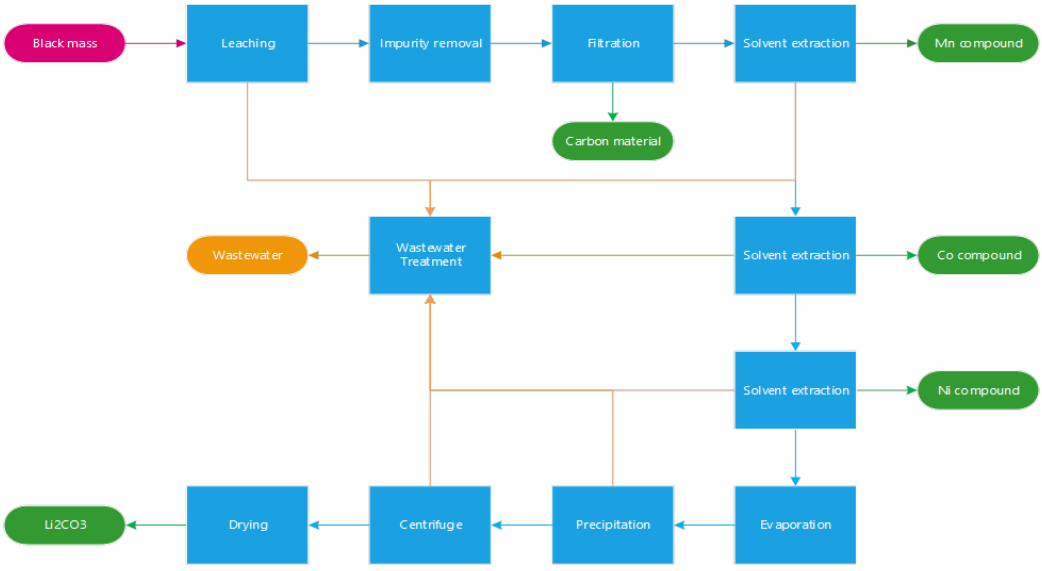

Figure 24: Process flow for the modelled generic pyrometallurgy-based recycling process according to EverBatt2023 [40].

7.7 Potential contributions to the climate change impact of producing 1 kg of LFP battery using recycled materials

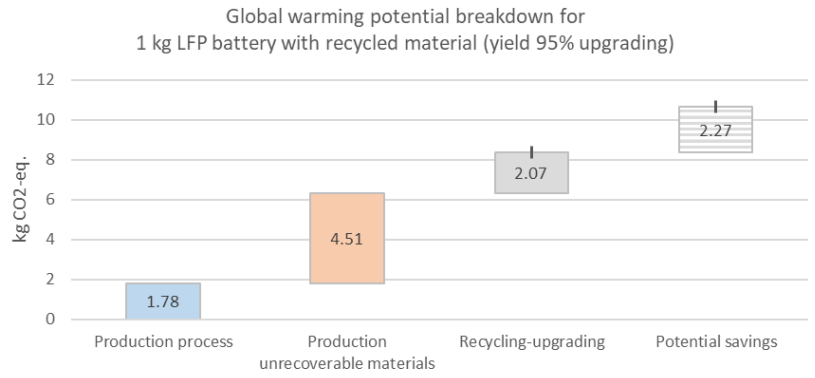

Figure 25: Potential contributions to the climate change impact of producing 1 kg of LFP battery using recycled materi-als, showing impacts from production processes, unrecoverable materials production, recycling/upgrading steps, and potential CO_2-equivalent savings. The figure is based on the assumption of a 95% yield for all the upgrading steps of the recovered materials.

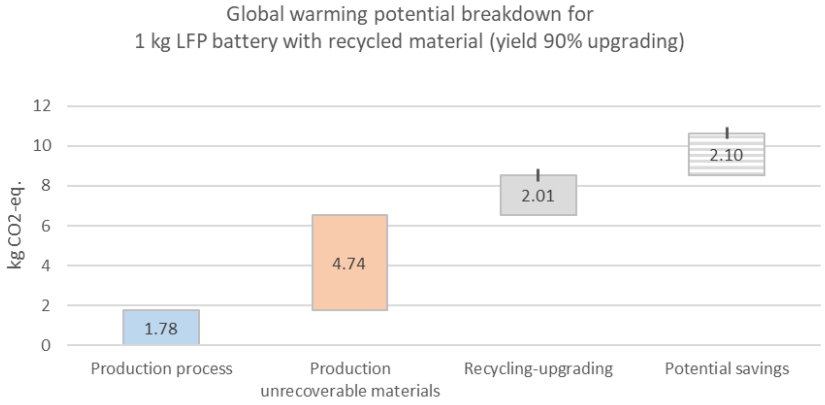

Figure 26: Potential contributions to the climate change impact of producing 1 kg of LFP battery using recycled materials, showing impacts from production processes, unrecoverable materials production, recycling/upgrading steps, and potential CO_2-equivalent savings. The figure is based on the assumption of a 90% yield for all the upgrading steps of the recovered materials.